Chem Soc Rev

Ultrafast and nonlinear surface-enhanced Raman spectroscopies

Journal:	*Chemical Society Reviews*
Manuscript ID	CS-REV-10-2015-000763.R1
Article Type:	Review Article
Date Submitted by the Author:	05-Jan-2016
Complete List of Authors:	Gruenke, Natalie; Northwestern University, Department of Chemistry Cardinal, Fernanda; Northwestern University, Department of Chemistry McAnally, Michael; Northwestern University, Department of Chemistry Frontiera, Renee; University of Minnesota, Chemistry Schatz, George; Northwestern University, Department of Chemistry Van Duyne, Richard P; Northwestern University, Department of Chemistry

Ultrafast and nonlinear surface-enhanced Raman spectroscopy

Natalie L. Gruenke[a], M. Fernanda Cardinal[b], Michael O. McAnally[c], Renee R. Frontiera[d], George C. Schatz[e], and Richard P. Van Duyne[f,*]

[a]*Department of Chemistry, Northwestern University, 2145 Sheridan Road, Evanston, Illinois 60208, United States. Tel: 847-491-2952; nlg@u.northwestern.edu*
[b]*Department of Chemistry, Northwestern University, 2145 Sheridan Road, Evanston, Illinois 60208, United States. Tel: 847-491-2952; fernanda.cardinal@northwestern.edu*
[c]*Department of Chemistry, Northwestern University, 2145 Sheridan Road, Evanston, Illinois 60208, United States. Tel: 847-491-2952; mcanally@u.northwestern.edu*
[d]*Department of Chemistry, University of Minnesota, 207 Pleasant St. SE, Minneapolis, MN 55455, United States.Tel: 612-624-2501; rrf@umn.edu*
[e]*Department of Chemistry, Northwestern University, 2145 Sheridan Road, Evanston, Illinois 60208, United States. Phone: 847-491-5657; schatz@northwestern.edu*
[f]*Department of Chemistry, Northwestern University, 2145 Sheridan Road, Evanston, Illinois 60208, United States.Phone: 847-491-3516; vanduyne@northwestern.edu*

*Corresponding author: Richard P. Van Duyne; vanduyne@northwestern.edu

ABSTRACT

Ultrafast surface-enhanced Raman spectroscopy (SERS) has the potential to study molecular dynamics near plasmonic surfaces to better understand plasmon-mediated chemical reactions such as plasmonically-enhanced photocatalytic or photovoltaic processes. This review discusses the combination of ultrafast Raman spectroscopic techniques with plasmonic substrates for high temporal resolution, high sensitivity, and high spatial resolution vibrational spectroscopy. First, we introduce background information relevant to ultrafast SERS: the mechanisms of surface enhancement in Raman scattering, the characterization of plasmonic materials with ultrafast techniques, and early complementary techniques to study molecule-plasmon interactions. We then discuss recent advances in surface-enhanced Raman spectroscopies with ultrafast pulses with a focus on the study of molecule-plasmon coupling and molecular dynamics with high sensitivity. We also highlight the challenges faced by this field by the potential damage caused by concentrated, highly energetic pulsed fields in plasmonic hotspots, and finally the potential for future ultrafast SERS studies.

Keywords: SERS, plasmonics, ultrafast spectroscopy, Raman scattering, TERS, SECARS, SEFSRS, TECARS

1. Introduction

Ultrafast surface-enhanced Raman spectroscopy is a growing field that uses plasmonic enhancements to study molecular motion and molecule-plasmon interactions on femtosecond and picosecond timescales. It utilizes the plasmonic enhancements observed in surface enhanced Raman scattering (SERS),[1, 2] which has achieved single molecule sensitivity[3-5] and sub-diffraction-limited resolution,[6-8] in combination with the time-resolution of ultrafast vibrational spectroscopy. The most recent advances in the field[9-12] have demonstrated the potential to watch single molecules react on the timescale of nuclear motion, positioning these techniques to answer long-standing mechanistic questions in plasmon-mediated chemical reactions.

By taking advantage of high enhancement factors and coherent signals, ultrafast SERS could be used to eliminate heterogeneity in dynamics studies, possibly achieving even higher sensitivity than spontaneous continuous wave (cw) SERS. This would allow, for example, for us to investigate how individual defect sites affect molecular dynamics of dye molecules on TiO_2-functionalized plasmonic substrates.[13] Ultrafast surface-enhanced Raman techniques could also prove instrumental in studying plasmon-driven chemistry, an emerging field probing phenomena such as hydrogen dissociation on gold nanoparticles.[14] Additionally, ultrafast SERS could be used to study the effects of plasmonic enhancement on electron dynamics in photovoltaic or photocatalytic materials, as reports have shown increases in efficiencies for plasmonically-enhanced systems without a clear consensus on the mechanism of these enhancements.[13, 15-18] Ultrafast SERS provides unique tools to study molecule-plasmon coupling in these systems, as well as to study dynamics near plasmonic surfaces on femtosecond timescales. In this paper, the term "ultrafast SERS" will be used generically for any Raman scattering process that involves ultrafast (picosecond or femtosecond) excitation and plasmonic enhancement, including nonlinear processes and related process such as sum frequency generation. This review discusses the growth of this field over the past few decades as well as recent advances that illustrate the power of ultrafast SERS techniques for future applications.

Ultrafast spectroscopy generally refers to timescales ranging from a few femtoseconds to hundreds of picoseconds, as these are the relevant timescales to follow vibrational molecular dynamics. Ultrafast spectroscopy has been used for decades to investigate molecular dynamics.[19, 20] By using a pump pulse followed by a probe pulse or pulses to investigate the electronic or vibrational state of the system at varying time delays, ultrafast spectroscopies are a unique and powerful tool for studying changes to systems on the extremely short timescales relevant to a large number of photochemical and photophysical processes. Ultrafast vibrational spectroscopies can provide more specific mechanistic information than complementary electronic spectroscopies such as transient absorption (TA) spectroscopy because they directly measure changes in nuclear motion on the actual timescales of the vibrations involved.[21] This vibrational information can reveal mechanistic details of reactions. For example, femtosecond stimulated Raman spectroscopy (FSRS) was used to map structural evolution during excited-state proton transfers in green fluorescent protein.[22] In addition to FSRS, a wide range of ultrafast Raman spectroscopy techniques have been developed over the past decades including time-

resolved resonance Raman, picosecond spontaneous Raman, coherent anti-Stokes Raman (CARS), and hyper Raman (HRS) spectroscopies. This review focuses on spectroscopies that have been successfully combined with plasmonic substrates for ultrafast SERS experiments.

In this paper we first provide the background information necessary to understand the growth of the ultrafast SERS field, including a discussion of SERS mechanisms and substrates, as well as a brief introduction to ultrafast spectroscopy of plasmonic materials and the growth of ultrafast Raman spectroscopies. We then review major advances in the field of ultrafast SERS and the challenges that have been overcome and still remain. Last we focus on ultrafast molecular plasmonics as an emerging field that holds promise to help us truly understand not only how molecules and plasmons interact but also how plasmons can mediate chemistry.

2. Background and Origins of Ultrafast SERS

In this section, we discuss the mechanism of SERS as well as implications of ultrafast electron dynamics in plasmonic materials for ultrafast molecular dynamics in coupled molecule-plasmon systems. We first introduce plasmonics and surface enhanced Raman scattering (SERS) along with the mechanistic details of plasmonic enhancements in Raman scattering relevant for ultrafast SERS. Next, we briefly discuss electron dynamics in plasmonic nanostructures and comment on early work that combines ultrafast vibrational spectroscopy and plasmons in order to lay the groundwork for a discussion of the ultrafast SERS field.

2.1 Plasmons and molecule-plasmon interactions

While we will mostly focus on plasmons as they related to SERS in this review, a basic understanding of the fundamental physics behind plasmonics is important to discuss the motivations and mechanisms for ultrafast SERS experiments.

Surface plasmons are the collective oscillations of conduction electrons in metal nanostructures, which can decay both radiatively and non-radiatively.[23] This collective oscillation can lead to local-field enhancements and strong extinction, as will be discussed in Section 2.2. The physics behind plasmon excitation and decay has been well-studied and reviewed elsewhere[23-27] and we only mention a few main points here to guide the reader. Briefly, after formation on the femtosecond timescale plasmons can decay through re-emission of photons (radiative) or energy transfer to electron-hole pairs to form hot electrons (non-radiative).[23, 28] Plasmons will dephase within tens of femtoseconds and thermalize via electron-electron scattering within hundreds of femtoseconds.[29] The hot electrons will relax on the time scale of picoseconds due to electron-phonon scattering followed by phonon-phonon interactions which cool the metal lattice after tens of picoseconds.[30-32]

When coupled with molecules, these plasmon dynamics are less clear. Molecule-plasmon interactions are not yet well-understood, though molecules could be affected in a number of

ways when placed in the proximity of excited plasmons. Molecules could be excited independently from the plasmon by incident irradiation, and their excited-state dynamics could be altered by the changing electromagnetic field caused by the decaying plasmon. Additionally, hot electrons generated from plasmon decay could react with coupled molecular systems and drive chemical reactions on ultrafast timescales. Section 2.4 further discusses molecule-plasmon coupling, and Section 5 outlines the potential of using ultrafast SERS techniques to study these phenomena. Most importantly for our purposes in this review, plasmonics are the dominant mechanism for the highly enhanced Raman scattering observed in SERS.

2.2 SERS: Mechanism, substrates, and hotspots

Surface-enhanced Raman scattering is a powerful tool to study molecular structure because it enhances otherwise weak Raman scattering by orders of magnitude.[1, 2, 33-41] Because of this enhancement, SERS is especially useful in sensing applications with sensitivity down to the single molecule level.[3-5] The enhancements observed in SERS arise mostly from the excitation of localized surface plasmon resonances (LSPRs) in noble metal nanostructures.[33] An LSPR arises from the collective oscillation of electron density relative to the metal nuclei in nanostructures significantly smaller than the wavelength of incident light, as illustrated in Figure 1a. This phenomenon results in a large electromagnetic enhancement of the incident and scattered fields involved in the Raman scattering process. Additional enhancement can come from the chemical enhancement mechanism, where the incident light excites charge transfer resonances between the metal and the adsorbed molecules.[42, 43]

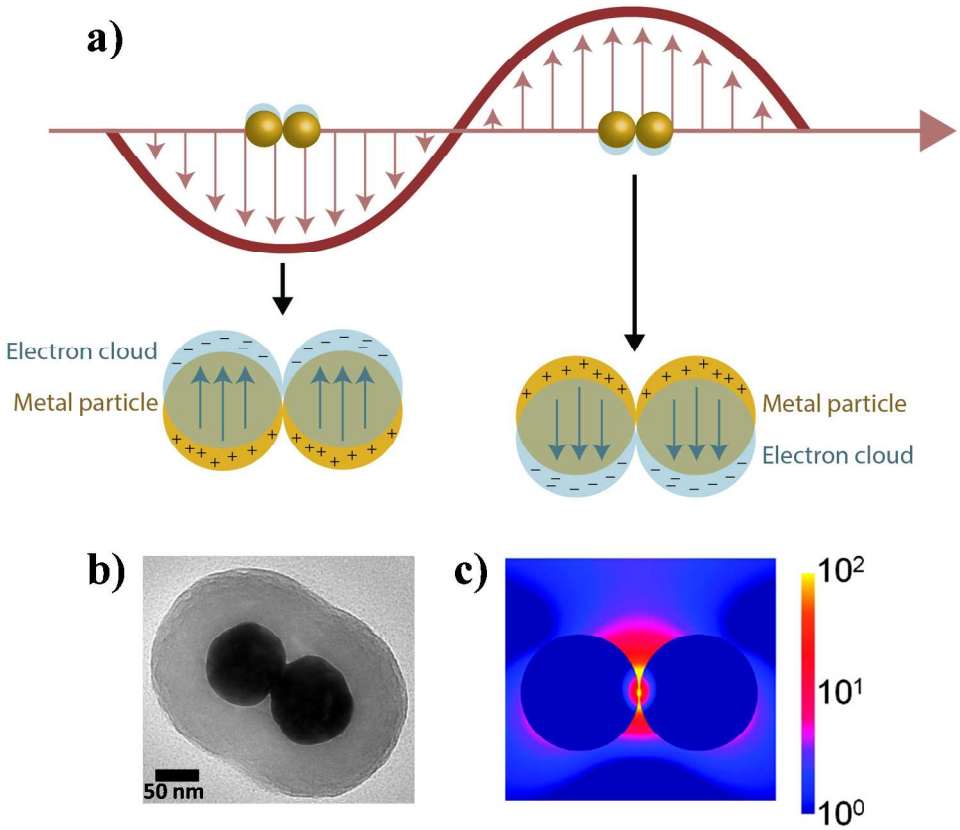

Figure 1. (a) Depiction of the electromagnetic SERS enhancement mechanism. (b) TEM of a gold dimer of 90-nm diameter particles encapsulated in 60 nm of silica. This is a common substrate used in ultrafast SERS measurements, with a small junction or gap where the particles meet. Reprinted with permission from reference [12]. Copyright 2012 American Chemical Society. (c) Illustration of a hotspot at the junction of a dimer aggregate of gold particles. FTDT calculations of the $|\mathbf{E}|^2/|\mathbf{E}_0|^2$ contour profiles show local field enhancements in the 0.5 nm gap between the two 100 nm particles, with yellow indicating areas of highest enhancement (hotspots). Reprinted with permission from reference [44]. Copyright 2012 American Chemical Society.

The increased signals seen in SERS are quantified by an enhancement factor (EF) that compares the surface-enhanced signal to the normal Raman scattering (NRS) signal (i.e. without a plasmonic substrate), normalized for the number of molecules probed. Enhancement factors provide a metric for directly comparing enhancement of different SERS substrates and experimental approaches. Specific definitions of EFs necessarily differ across applications,[45] for example surface-enhanced coherent anti-Stokes Raman scattering (SECARS) enhancements have been compared to both NRS and CARS. However, the direct comparison of EF values is further complicated by the fact that not all authors use the same EF calculations even for similar applications. In general, enhancement factors should compare plasmonically enhanced scattering to unenhanced scattering, normalized for the number of molecules contributing to each of the observed signals (along with any other experimental variables changes between SERS and NRS acquisitions). A typical enhancement factor formula used is shown in Equation 1

$$EF = \frac{I_{SERS}/N_{Surf}}{I_{NRS}/N_{Vol}}$$

where I_{SERS} is the intensity of the SERS signal, N_{Surf} is the number of molecules on the surface of the SERS substrate that are contributing to the SERS signal, I_{NRS} is the intensity of the NRS signal, and N_{Vol} is the number of molecules in the focal volume contributing to the NRS signal. The electromagnetic enhancement mechanism can lead to EFs of 10^4-10^8 (with theoretical predictions up to 10^{11}),[46] resonance Raman effects can yield 10^3-10^6 enhancement,[47] and chemical enhancement[43] can add an additional enhancement of 10-100 for observed experimental enhancement factors of up to 10^{11}.[48] Taking advantage of these enhancements, SERS has been used for the past 40 years for biosensing applications,[49] spectroelectrochemistry,[50] cultural heritage applications,[51] and single molecule spectroscopy.[3, 4, 48]

For Raman enhancement in the visible and near infrared (NIR), gold and silver nanostructures yield the highest enhancement factors due to their dielectric properties.[35, 52] Common SERS substrates include colloidal solutions of nanoparticles, nanostructured films or electrodes, isolated nanostructures on a substrate, or arrays of coupled nanostructures.[35, 52] Ultrafast SERS experiments have utilized a number of substrates, mostly colloidal solutions of aggregated particles, single aggregates of particles, and arrays of coupled nanostructures. The plasmonic enhancements in SERS are highest in so-called plasmonic hotspots in small gaps between nanostructures or at particularly sharp nanoscale features (see Figure 1b,c).[35, 44, 53] All of the major successes in the implementation of ultrafast SERS have utilized substrates with hotspots between nanoparticles or hotspots between a plasmonic scanning probe microscope (SPM) tip and a substrate (known as tip-enhanced Raman spectroscopy or TERS). These hotspots not only yield high enhancement factors, but also provide spatial localization of the Raman signal for domain sizes smaller than the diffraction limit. TERS, for example, can be used to study molecules between a plasmonic tip and a plasmonic film with spatial resolution well below 10 nm. In this way, plasmonic hotspots can be used not only to study a small number of molecules near nanostructures (even single molecules for highly-enhancing substrates), but also to obtain spatial resolution below the diffraction limit. These advantages lead the way for powerful ultrafast SERS applications if ultrafast time resolution can be combined with high sensitivity and sub-diffraction spatial resolution.

2.2 Ultrafast plasmonics: electron dynamics in metal nanoparticles

The electromagnetic field enhancement resulting from excitation of LSPRs is typically the major contribution in the overall Raman signal augmentation in SERS. Therefore, understanding how the LSPR, electric field confinement, and plasmon-molecule interactions are affected by ultrafast irradiation is central for the development of ultrafast Raman spectroscopies. Fundamental understanding of ultrafast molecular plasmonic systems is essential for the applications of nanotechnology in varied fields such as medicine,[54, 55] catalysis,[14, 56, 57] and energy;[58] and has remained challenging. During the last two decades, substantial progress has been made independently in the fields of Raman spectroscopies, molecular dynamics and electron dynamics in plasmonic structures.

The importance of electron dynamics in the context of this review is to understand the processes that can be caused by an ultrafast laser pulses impinging on metallic nanostructures. Specifically, the time dependent optical response of the metal nanostructure (transient extinction or absorption) and the associated energy transfers that can alter molecule-substrate interactions in time-resolved ultrafast Raman spectroscopies.

Ultrafast pump-probe spectroscopy can probe a wide range of phenomena, including electron dynamics and material properties.[59-65] Pump-probe spectroscopy involves two ultrafast laser beams, a pump beam to excite or perturb the sample out of an equilibrium state, and a probe beam used to monitor the pump-induced changes of the optical properties over time. In pump-probe experiments involving metallic nanostructures the transient extinction, absorption, or scattering signals can be monitored upon excitation.[59, 61, 62, 66, 67] In this case, the lattice of the metallic nanostructure and its environment are indirectly heated since the absorbed energy is first redistributed among the electrons by electron-electron (e-e) scattering, raising the electron gas temperature, then transferred to the lattice by electron-phonon (e-ph) interaction on a subpicosecond time scale.[66] Electron-electron and electron-phonon scattering are coupled processes.[62, 66] After electron-phonon scattering, the raised lattice temperature causes expansion and thermalization by acoustic vibrational modes where energy is exchanged with the environment.[62, 66] These vibrations typically take place within few to tens of picoseconds, and complete thermalization with the environment takes longer times (>100 ps) depending on the particle material, size and surrounding medium (see Figure 2).[62, 66, 68] The lattice vibrations triggered by the e-ph interaction modify the metallic nanoparticle density and optic properties; and the thermalization process modifies the refractive index of the environment; these changes produce the transient signal (see Figure 2, and inset of Figure 3).

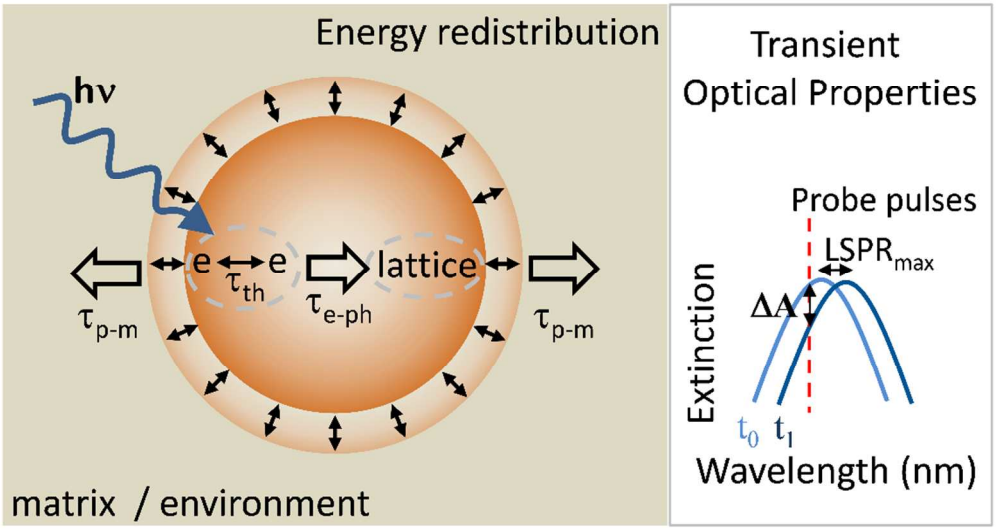

Figure 2. Left: Scheme of energy redistribution in a metal nanoparticle after electrons are selectively excited by a femtosecond pulse (hυ). Each process has characteristic time scales; for internal thermalization of the electron gas, τ_{th} is of the order of femtoseconds; for electron-lattice thermalization, $\tau_{e\text{-}ph}$ is of few to few tens of picoseconds and for particle-matrix energy exchanges, $\tau_{p\text{-}m}$ is larger than tens of picoseconds.[62, 66] Adapted

with permission from reference [66]. Copyright 2001 American Chemical Society. Right: Sketch illustrating the transient optical properties monitored in a pump-probe experiment (ΔA), which can be understood as changes in the dielectric function of the metallic nanoparticle due to hot electrons and hot lattice thermalization.

Most of the plasmonic nanostructures studied by transient absorption refer to colloidal dispersions[69-78] or isolated single particles dispersed on a substrate or matrix.[79-85] Colloidal aggregates or nanostructures with hotspots are less frequently studied by transient absorption. However, these plasmonically coupled systems are more interesting for SERS applications due to their higher field enhancements. There are conflicting reports studying gold particle pairs where it is observed that lattice vibrations are influenced by the near-field coupling,[86] and others where they are not.[87, 88] An example of the former case was reported by Lippitz and coworkers who studied a pair consisting of 40 nm and 70 nm gold disks, separated by a small gap of ~15 nm. In their work, the 70 nm disk acts as an antenna, increasing the transient absorption signal amplitude of the smaller particle. The pump pulse excited both disks in the pair and the probe pulse was polarized whether along the symmetry axis of the pair to study strong coupling (upper row Figure 3), or perpendicularly to study weak coupling (lower row Figure 3). The insets of Figure 3 show examples of transient absorption measurements, where the relative transmission (ΔT/T) is monitored as a function of the relative time delays of the pump and probe pulses. Lippitz and coworkers used Fourier transformation to analyze the experimental data in the frequency domain, and in the case of strongly coupled disks (i.e. probe polarized parallel to the symmetry axis) they observed two peaks at 22 and 36 GHz and assigned them to the 70 nm and 40 nm disks respectively. Additionally, the amplitude of those peaks varied similarly in shape and position as a function of the probe wavelength (see Figure 3c), confirming plasmonic coupling in agreement with simulations. Distinctly, when the probe pulse was polarized perpendicular to the pair symmetry axis, the Fourier transform showed only the 22 GHz peak of the 70 nm disk (Figure 3b), and the amplitude dependency to the probe wavelength (Figure 3d) suggested an uncoupled large disk according to simulations. Hence, the antenna enhancement on the small disk was controlled by the probe polarization.[86] Another plasmonically coupled nanostructure system was studied by Large et al. using transient absorption and resonant Raman scattering. The authors compared coupled silver particles aligned into columns to smooth columns of silver without any hotspots; and the authors observed strong enhancement of the acoustic vibrational modes of the coupled nanostructure only. In other words, when the excitation polarization was chosen to excite the hot spots, a new acoustic vibration band was experimentally observed that was only theoretically predicted for the coupled nanostructure, and not for a smooth column.[89] These ultrafast transient absorption studies demonstrated unique features in the electron dynamics of plasmonically coupled substrates, similar to nanostructures used in ultrafast SERS studies.

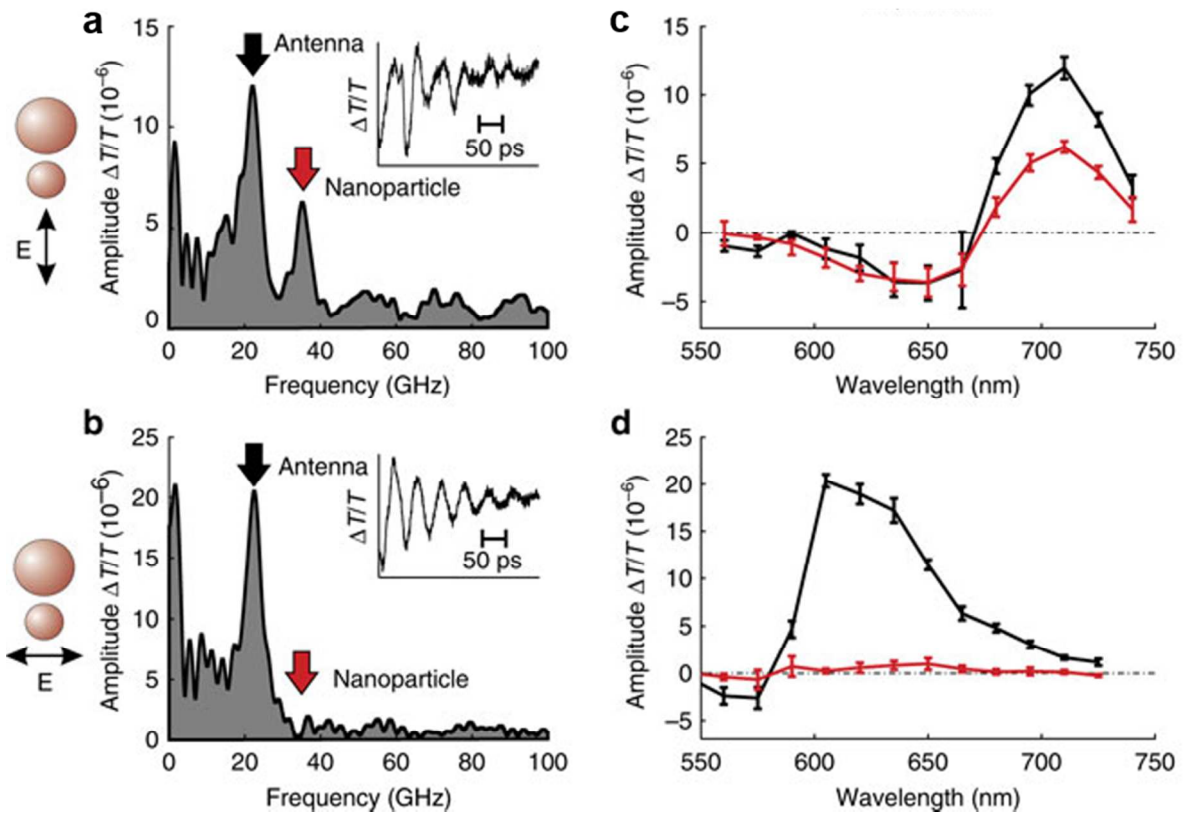

Figure 3. Transient absorption studies on a pair of gold disks of 40 and 70 nm, where the larger acts as an antenna. In this nanostructure, the polarization of the probe light determines the coupling strength between the disks. The upper row (a, c) shows the strong antenna-nanoparticle coupling case, as the probe pulse is polarized along the symmetry axis of the structure. The lower row (b, d) shows the weak coupling case, when the polarization of the probe is perpendicular to the symmetry axis of the pair. The response of the 40 nm particle and of the antenna (70 nm) are drawn in red and black, respectively. The insets in a and b are examples of transient transmission traces, monitoring the lattice vibrations at their maximum signals obtained with 800 nm pump pulses and 710 nm and 605 nm probe pulses, respectively (a,b). The Fourier transformation of such transient transmission traces (a, b) show a mode at 22 GHz which was assigned to the vibrational response of the antenna; and only in the strong coupling case (a) a mode at 36 GHz which was assigned to the 40 nm nanoparticle based on theoretical predictions. The oscillations amplitude dependency to the probe wavelength are shown in c and d; and in the first one both modes vary similarly in amplitude and shape, suggesting again strong correlation between them. The error bars show the standard deviation. The line is a guide to the eye. Adapted from reference [86]. Copyright © from 2011 Macmillan Publishers.

These ultrafast transient absorption studies demonstrated unique features in the electron dynamics of plasmonically coupled substrates, similar to nanostructures used in ultrafast SERS studies; emphasizing the dynamic nature of LSPR resonances and hot spots, and their possible interactions with interfacial molecules on the femtosecond time scale.

2.3 Molecule-plasmon interactions and the origins of ultrafast Raman spectroscopy

As was demonstrated in the previous section, it is important to study the ultrafast dynamics of molecules and plasmonic SERS substrates as a coupled system and not independently. The effect of plasmonic substrates on coupled molecular dynamics is not yet well-understood for many reactions and nanostructures.[56, 57, 90] Therefore studying plasmonic influences on analyte molecules could help inform an overall understanding of molecule-plasmon interactions in ultrafast SERS. Here we discuss some relevant studies.

There is now clear evidence for strong interactions between a localized surface plasmon resonances and a molecular transition when the molecules are in close proximity to a nanostructured surface.[56, 57, 91-96] For example, this has been clearly demonstrated in several studies addressing the interaction of molecular excitons of J-aggregates and plasmonic nanostructures.[97-109] Molecular excitons are electron–hole pairs bound by the Coulomb potential and when coupled to metal nanoparticles, the excitation may not be purely molecular.[98] For example, Wiederrecht and coworkers investigated silver nanoparticle/cyanine J-aggregate hybrid systems and observed reversible photoinduced charge transfer with silver nanoparticles that does not take place on the bulk metal where the exciton is quenched.[99] Also, the authors investigated the coherence of such interaction for gold and silver nanoparticles observing that the excitons of J-aggregate coated metal nanoparticles were coupled coherently to the dipolar responses of both metals but in different ways; highlighting the importance of the plasmonic material involved.[100] Strong plasmon-exciton coupling might result in anticrossings of the hybrid plexcitonic (i.e., mixed exciton-plasmon) dispersion curves and the formation of two hybrid energy states separated by a Rabi splitting energy.[102, 103, 110] This is illustrated in Figure 4, that includes studies of cyanine dye (TDBC) J-aggregates coupled to silver nanoprism plasmons at ambient conditions.[102] Figure 4a shows the optical properties and chemical structure of the TDBC molecule, Figure 4b shows the scattering spectrum for a single silver nanoprism, and then Figure 4c illustrates the effect of coupling both. In Figure 4c, the scattering spectrum of such coupled plasmon-exciton system shows a dip between two branches (ω_+ and ω_-), that is the Rabi splitting. Interestingly, upon laser-induced degradation of the molecular J-aggregate, the plasmon-exciton coupling gradually disappears (see Figure 4d). These observations highlights the optical consequences of molecule-plasmonic interactions, and is especially relevant to degradation observed in ultrafast SERS experiments (as will be discussed in section 4).[102]

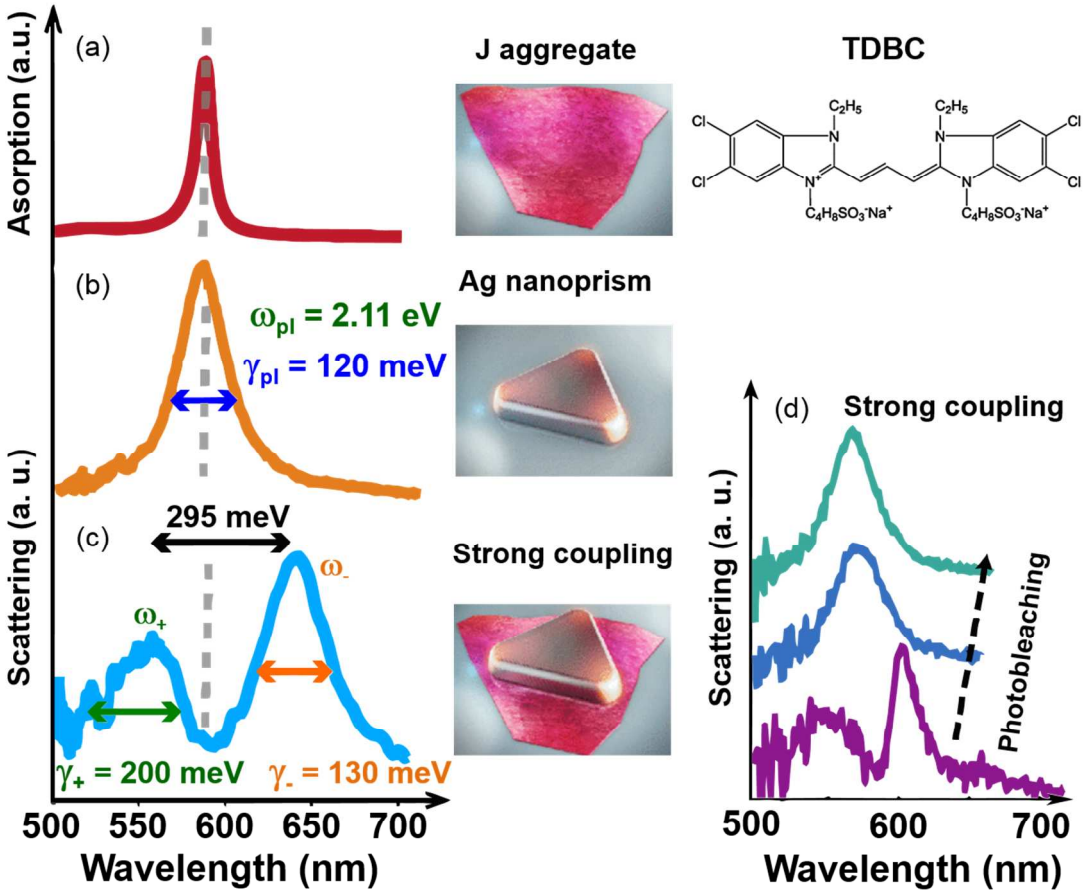

Figure 4. Example of molecular excitons and nanoparticle plasmon coupling. (a) Extinction spectrum of TDBC J aggregates in water, scheme of a J-aggregate sheet and TDBC molecular structure. (b) Scattering spectrum of a bare silver nanoprism with the plasmon resonance energy (ω_{pl}) and its full width at half maximum (γ_{pl}). (c) Scattering spectrum of single nanoprism strongly coupled to J aggregates, resulting in a pronounced scattering dip and hybrid plasmon-exciton branches (ω_+ and ω_-). (d) Scattering spectra of a strongly coupled plasmon-exciton system with a Rabi splitting -dip in purple trace-, that vanishes away after molecular degradation. Adapted from reference [102]. Copyright American Physical Society 2015.

Time-resolved techniques, other than transient absorption, have also been used to study the interaction of molecules with SERS active substrates.[111-113] For example, Sawada and coworkers used transient reflecting grating to investigate the SERS response of various chemisorbed molecules on gold nano-roughened substrates. Sawada and coworkers found that the SERS response was dependent on electron transfer from the excited state of gold to the adsorbed molecules. More precisely, a larger number of charge transfer electrons would trigger a larger SERS band enhancement. This finding helped to support the basis of the chemical mechanism of SERS, mentioned in Section 2.2.[111, 112]

An alternative way of evaluating how ultrafast lasers could alter SERS signals is by studying vibrational pumping. Vibrational pumping refers to the increase in higher excited vibrational state population due to SERS Stokes scattering.[114] It has been reported that

vibrational pumping is observed when anti-Stokes to Stokes SERS intensity ratios are higher than those predicted by Boltzmann distribution with increasing excitation power.[115, 116] However there is controversy concerning the mechanism causing vibrational pumping and the roles of Raman scattering[114] and electronic excitation.[116] Kozich et al. addressed this question with sub-picosecond time resolved SERS spectra of Rhodamine 6G in a colloidal silver solution. Kozich et al. estimated the vibrational excess populations accumulated for the different modes of Rhodamine within the pulse duration by comparing ps pulsed and cw excitations.[116] To monitor the temporal evolution of vibrational populations the authors applied a one color (i.e. one wavelength) pump-probe SERS scheme. The pump-probe anti-Stokes SERS spectra were recorded for different delay times and the spectrum recorded at a delay time of 15 ps was subtracted from the rest as a reference. In the difference spectra, the intensity of the three main bands reaches a maximum for a delay time of 1 ps and then decays. From the observed temporal evolution of the anti-Stokes to Stokes SERS intensity ratio, the authors determined that the population of Raman-active modes at higher frequency was more enhanced compared to calculated thermal population distributions and concluded that the electronic excitation causes the vibrational pumping.[116] These results support the development of ultrafast Raman spectroscopies and show that time-resolved investigations are advantageous for mechanism evaluation and overall understanding of molecule-plasmon interactions under pulsed irradiation.

Modulation techniques are frequently employed in ultrafast studies and Raman spectroscopic measurements to improve signal to noise ratios (SNR). For example, stimulated Raman gain[117] and Kerr gating[118, 119] techniques can enhance sensitivity by suppressing fluorescent background. In 1999, Matousek and coworkers demonstrated the effectiveness of picosecond Kerr gating for fluorescence background rejection by measuring the time-resolved spectra of p-quaterphenyl from solutions contaminated with a fluorescent dye [118] as well as by following the dynamics of the intramolecular charge transfer state of 4-dimethylaminobenzonitrile in unleaded petrol.[119] In 1979 Levine et al. proposed to use stimulated Raman gain for studying surface vibrational spectroscopy with an optimized experimental set-up.[117] This approach involved picosecond pump and probe beams synchronously mode-locked, with amplitude and frequency modulations to maximize the signal-to-noise ratio. The authors successfully detected the Raman gain spectrum of p-nitrobenzoic acid on a thin film of plasmonically-inactive alumina[120] as well as submonolayer coverage of a resonant Raman probe, [117] which evidenced this approach as a promising way of following molecule-substrate dynamics.

To conclude this section, we would like to reinforce that electron dynamics of isolated metallic nanostructures are strongly related to the plasmon resonance of the system as was shown in the pump-probe transient extinction experiments discussed in Section 2.3. In molecule-plasmon coupled systems, molecular transitions can be affected in varied degrees by the plasmonic nanostructure; where often the molecular and plasmonic electron dynamics mutually affect each other. Finally, in order to study coupled molecule-plasmon systems with vibrational spectroscopies, ultrafast techniques including pulse polarization, frequency, and amplitude modulation, such as Kerr gating and stimulated Raman gain, are

advantageous. These advances demonstrated the power of ultrafast Raman spectroscopies as well as important dynamics to consider in coupled molecule-plasmon studies.

3. Ultrafast SERS and related techniques

One of the major aims of ultrafast spectroscopy is to study molecular dynamics by tracking nuclear and electronic motion, as well as the coupling of these motions, on their inherent timescales. An important question has been whether these dynamics can be observed on the single molecule level. Towards this goal, a number of approaches have been developed that combine the molecular sensitivity provided by SERS with the time-resolution of ultrafast spectroscopy. These surface-enhanced ultrafast vibrational spectroscopies not only work towards the limit of watching single molecules react in real-time, but also allow us to study unique dynamics near plasmonic surfaces for application in plasmonically-enhanced photovoltaics and catalysis as well as in plasmon-mediated chemistry.

The enhancement observed in spontaneous surface-enhanced Raman spectroscopy has been applied to many non-linear processes including second harmonic generation, sum frequency generation, hyper-Raman scattering, coherent anti-Stokes Raman scattering, and femtosecond stimulated Raman scattering. Figure 5 provides a guide to the differences in these vibrational spectroscopies using energy diagrams to help illustrate the pulses and resonances used. In this section we discuss advances in combining surface-enhancement from plasmonic materials with ultrafast vibrational spectroscopy of molecules. We focus on highlighting the most successful ultrafast surface-enhanced Raman and related spectroscopic techniques for an in-depth discussion of what this field has accomplished.

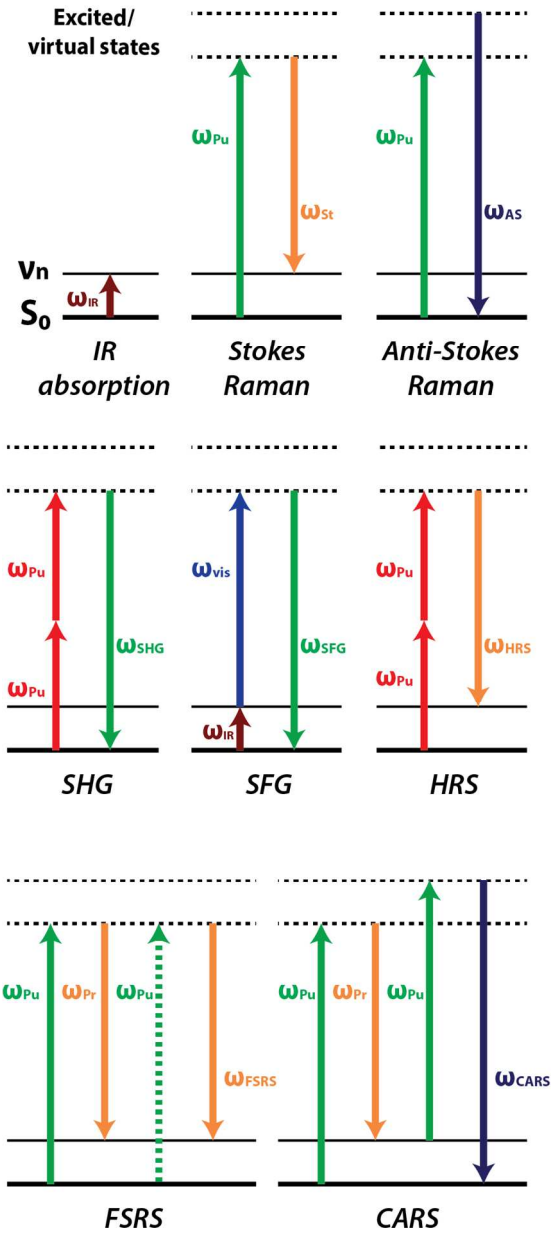

Figure 5. The above diagrams depict the different energies of photons and interactions used for the vibrational spectroscopies discussed in this section. S_0 refers to the ground state, v_n is a real vibrational state, and the top dashed lines depict either real or virtual states depending on resonance conditions. The colored arrows depict interactions labeled as ω_{IR} for infrared (IR) absorption, ω_{Pr} for probe interactions, ω_{Pu} for pump interactions, ω_{St} for Stokes shifted frequencies, ω_{AS} for anti-Stokes shifted frequencies, ω_{SHG} for second harmonic generation (SHG), ω_{SFG} for sum frequency generation (SFG), ω_{FSRS} for femtosecond stimulated Raman scattering (FSRS), and ω_{CARS} for coherent anti-Stokes Raman scattering (CARS).

3.1 Surface-enhanced sum frequency generation (SFG) and second harmonic generation (SHG)

The first surface-enhanced ultrafast spectroscopies that we will discuss are not exclusively Raman spectroscopies, but techniques that rely on Raman scattering and are therefore similarly enhanced with plasmonic substrates. Just as SERS provides vibrational information and dynamics for surface adsorbates or molecules near plasmonic surfaces, sum frequency generation (SFG) is a powerful tool for investigating interfaces.[121-123] SFG involves a visible beam and an IR beam that are temporally and spatially focused at an interface. The SFG signal results from a coherent combination of an infrared and a Raman transition of the molecules at the interface; with light emitted at the sum frequency of those transitions, as indicated by the energy diagram for SFG in Figure 5. Second harmonic generation (SHG) is a more specific form of SFG in which both incident photons are equal in energy (and thus the resulting SHG is twice the frequency of the incident photons). Though SHG is not a Raman scattering technique, we briefly mention it here in relation to SE-SFG experiments as they often are associated. Since SFG is an inherently nonlinear coherent spectroscopy that is $\chi^{(2)}$ in nature it is generated only from a medium with a lack of inversion symmetry and thus is ideally suited to overcome sensitivity issues when attempting to selectively study the dynamics of a small number of molecules on a surface or at an interface (where symmetry is broken). Thus a number of SHG and SFG studies have been done on metal substrates, most without taking advantage of plasmonic enhancements.[124, 125] However, nanostructured plasmonic surfaces can be used to enhance often weak molecular SFG and SHG signals for higher sensitivity and potentially the study of molecule-plasmon interactions. In this section we will briefly discuss examples of SE-SFG and SE-SHG of molecular species on plasmonic surfaces.

The first demonstrations of SE-SHG of molecular analytes was by Chen et al. in the early 1980's.[126] They compared SERS and SE-SHG of silver cyanide and silver chloride adsorbates on roughened silver electrodes, finding that both the Raman and SHG processes were enhanced by the plasmonic substrate. They reported enhancements of 10^4 for SERS and 10^2 for SE-SHG. The significant difference between these processes was attributed to the fact that SE-SHG is inherently more sensitive to the molecular orientation and symmetry due to the requirement of a lack of inversion symmetry for signal generation. Using pulses of ~10 ns in duration, these results served as a proof-of-principle study for future ultrafast SE-SFG experiments decades later.

One of the first uses of ultrafast SE-SFG to plasmonically enhance molecular signatures was in the Benderskii group.[127, 128] They used broadband femtosecond infrared and narrow-band picosecond visible laser pulses to perform vibrational SFG studies on gold nanoparticles of varied sizes (from 1.8 to 25 nm) functionalized with dodecanethiol. Since SFG is a sensitive probe of surfaces, even without plasmonic enchantments, detection of dodecanethiol SFG spectra was possible at a few percent of a monolayer on nanoparticles surfaces. Their results indicated that there is a dependence of the molecular conformation of the ligand (dodecanethiol) on the nanoparticle size. These experiments indicated the power of SE-SFG for the study of ultrafast plasmonics due to its sensitivity to molecular configuration, which could play major role in plasmon-mediated reaction pathways.

Additional advances were made by Pluchery et al., who measured enhancement factors of 21 for the SFG signal from thiophenol on gold nanoparticles compared to

Au(111) surfaces.[129] Thus they demonstrated that SE-SFG allowed not only for the study of molecular adsorbates with surface specificity but also a direct chemical probe of capping layers on the surface of nanoparticles. Towards the goal of studying reaction dynamics using SE-SFG, Beladelli et al. were able to study the absorption of CO on platinum nanoparticle arrays compared to thin films.[130] They measured enhancements of ~10^4 for CO adsorbed at 1 atm on nanoparticles of 45-nm diameter, paving the way to study catalytic reactions under typical reaction conditions. Similar enhancement factors have been reported by Tsuboi et al., with EFs of 3x 10^5 for the enhancement of SHG from gold nanospheres immobilized by amine terminated self-assembled monolayers on a gold surface.[131] A number of other studies have used plasmonic substrates to enhance SFG signals, but have observed enhancement factors of only one or two orders of magnitude or did not explore the magnitude or mechanism of plasmonic enhancements at all.[132-134] Thus, while the enhancement factors for SE-SHG and SE-SFG tend to vary by orders of magnitude, it is clear that the power of this inherently surface-selective technique can be combined with the sensitivity provided by plasmonic enhancements in order to study molecular dynamics in the future.

3.2 Surface-enhanced hyper Raman scattering (SEHRS)

Hyper-Raman scattering (HRS) is an inelastic sum-frequency scatter from two photons, distinct from normal Raman scattering (NRS) which results from scattering of a single photon. As depicted in Figure 5, two photons at frequency ω inelastically scatter from a ground state to a virtual state with energy equal to $2\omega - \omega_{vib}$ corresponding to Stokes scattering (or $2\omega + \omega_{vib}$ corresponding to anti-Stokes scattering). HRS is an intrinsically weak process with scattering cross-sections on the order of ~ 10^{-60} cm^2, comparable to the product of two linear NRS events and commonly uses ultrafast pulsed lasers to drive the HRS process with high peak powers.[135] The low HRS cross-sections result in weak transition probabilities, requiring enhancement to provide sufficient signal-to-noise for identifying molecular signatures. One method of enhancement uses molecular electronic resonance: resonant hyper-Raman scattering (RHRS) where a molecular electronic transition corresponds to the sum frequency of the incident photons. A second method that is often used with resonant enhancement is surface-enhancement (SE-) which leads to large enhancement factors on the order of 10^{10} – 10^{14} over non-plasmonically enhanced nonresonant HRS.[136, 137] While the field of HRS is diverse,[138] we will focus specifically on surface-enhanced hyper-Raman scattering (SEHRS) that is done with picosecond and femtosecond pulsed lasers to drive the nonlinear surface-enhanced Raman process.

The first SEHRS spectra obtained with picosecond excitation was from the Van Duyne group in 1988.[139] This early report of SEHRS is one of few that contain both experiment and theory for the vibrational assignments. Experimentally, the group observed SEHRS of pyridine on a roughened silver working electrode. This study showed an enhancement factor of 10^{13} for SEHRS compared to bulk HRS.[139] These results demonstrated that SEHRS could be a useful technique combining ultrafast pulses and surface-enhanced Raman.

An early report of SEHRS with picosecond pulses came from the Yu group at the Georgia Institute of Technology in early 1990.[140] The Yu group reported effects of pulse

compression in resonant and non-resonant surface-enhanced hyper-Raman scattering to demonstrate the feasibility of SEHRS using lower-average-power laser systems. For SEHRS of basic fuchsin and 3-hydroxykynurenine in Ag colloidal solutions, the Yu group observed increased SEHRS intensity by factors of 7 and 11 in the resonant and nonresonant cases respectively after compressing the pulses from 100 to 5 picoseconds at an 82 MHz repetition rate and only 0.1 W of average power.[140]

After this initial work, SEHRS was extended to a variety of strong Raman scatterers including Rhodamine 6G (R6G), crystal violet (CV), and $Ru(bpy)_3$ in Au,[141] Ag,[137, 142] and Cu colloidal solutions.[141] Interestingly, in a Ag colloid – CV analyte system, the electromagnetic contribution to SEHRS was determined to be greater than SERS by six orders of magnitude.[142] Using the same Ag-CV system, the Seifert group studied two-photon resonant and pre-resonant conditions in SEHRS to examine wavelength dependence of the plasmonic enhancement and observed an estimated maximum total enhancement factor of 10^{14} for SEHRS compared to normal Raman scattering.[137] The electromagnetic enhancement factors observed in SEHRS suggest higher electromagnetic enhancement factors can be attained by introducing more laser – molecular plasmonic system interactions in higher order nonlinear spectroscopies. This idea is further explored by the SECARS and SE-FSRSprocesses, to be discussed later in Sections 3.3 and 3.4 of this review. The SEHRS results also demonstrate the potential for ultrafast SERS techniques not only to study complex reaction dynamics, but also as a mechanism for sensitivities even higher than can be achieved with SERS.

The SEHRS field has moved past initial proof-of-principle experiments to begin exploring the limits and potential applications of the technique. Recently, the Camden group achieved single molecule sensitivity[136] and characterized single-photon forbidden excited states.[143] Using a Ag-CV colloid system, a conclusive proof of single molecule sensitivity was obtained by observing separate deuterated and non-deuterated CV isotopically labeled vibrational spectra.[136] To observe an optically dark electronic state in NRS, SEHRS can be used due to the weaker selection rules and two-photon resonant condition. Using SEHRS in a wavelength scanned experiment, they characterized the excited state vibrational modes of R6G from three singlet excited states: S_1, the one-photon inaccessible S_2, and S_3.[143] With these results, the Camden group not only demonstrated the high sensitivity of SEHRS as an nonlinear SERS technique using ultrafast pulses, but also its potential application for the study of excited states.

SEHRS has also explored the applicability of nonlinear SERS techniques to biologically-relevant applications. Due to the two-photon resonant condition of SEHRS, wavelength dependent features of complex media can be exploited, such as the limited laser excitation and signal detection transmission ranges in biological samples. An early biologically relevant SEHRS study was performed by the Kneipp group where they recorded SEHRS of amide I and II stretches and DNA C-O stretches.[135] This was the first foray into using SEHRS as a vibrational spectroscopy analog to two photon fluorescence for molecular characterization in cells. To further push SEHRS for biological applications, the Camden group used short-wave infrared (SWIR) excitation to perform SWIR hyper-Raman microscopy.[144] The SWIR region for excitation has numerous advantages in biological microscopy studies as the wavelength has demonstrated vastly improved

penetration depth in comparison to the more common 800 nm excitation using in microscopy.[145] In addition, the wavelength of the SEHRS scattering is in a region that is weakly absorbed.[135, 137, 142] Using SWIR microscopy, the Camden group observed SEHRS of R6G and benzenethiol on silver colloids to demonstrate the use of SEHRS for future biological applications.[144]

SEHRS has expanded from its beginnings as a proof-of-principle second order nonlinear Raman scattering process.[140, 141] This nonlinear SERS technique has combined ultrafast pulses and plasmonic enhancements to characterize biological samples, [135 144] one-photon forbidden electronically excited states,[143] and single molecule-plasmon aggregates.[136] The future of SEHRS as a useful spectroscopic and microscopic technique will depend on applying its unique second-order nonlinearity,[138, 146] multiphoton plasmonic enhancement,[141] and intrinsic frequency doubling to take advantage of wavelength dependent extinction in complex media.[144] SEHRS's strength as a nonlinear SERS technique is that is uses plasmonic enhancements for extremely high sensitivity in what would otherwise be a useful, but weak process.

3.3 Surface-enhanced coherent anti-Stokes Raman scattering (SECARS)

One of the early attempts at improving weak Raman scattering for vibrationally sensitive molecular spectroscopy was coherent anti-Stokes Raman scattering (CARS).[147] CARS is a nonlinear Raman scattering process that is third order ($\chi^{(3)}$) in nonlinear polarization and has advanced rapidly over the years for spectroscopic and imaging applications. [148-151] The broad literature for CARS has been well reviewed previously[152-154] and for the purpose of this review we focus solely on CARS experiments that combine the CARS process with plasmonic enhancement of the exciting and/or signal fields.

3.3.1 CARS

A typical CARS experiments utilizes pump (ω_{pu}) and Stokes (ω_{St}) fields which interact in a media, creating a third order nonlinear polarization CARS signal (ω_{AS}). When the frequency difference of the pump and Stokes fields match the frequency of a Raman active mode, the Raman mode is coherently driven by the excitation fields. The resonantly driven Raman mode generates a new field that is spectrally removed from the excitation fields as an anti-Stokes shift from the pump field at $\omega_{AS} = 2\omega_{pu} - \omega_{St}$.[152] Since signal generation is dependent on selection of incoming beam frequencies, phase matching conditions of the excitation and signal fields are used to maximize CARS signal, as diagrammed in Figure 7a. The phase-matching conditions in CARS are typically met by one of three experimental conditions: a collinear geometry with proper frequencies of the excitation fields; spatial arrangement of excitation fields, most typically a BOXCARS arrangement (Fig. 7b); or high numerical aperture (high-NA) focusing conditions, like that in a microscope (Fig. 7c).[152, 155]

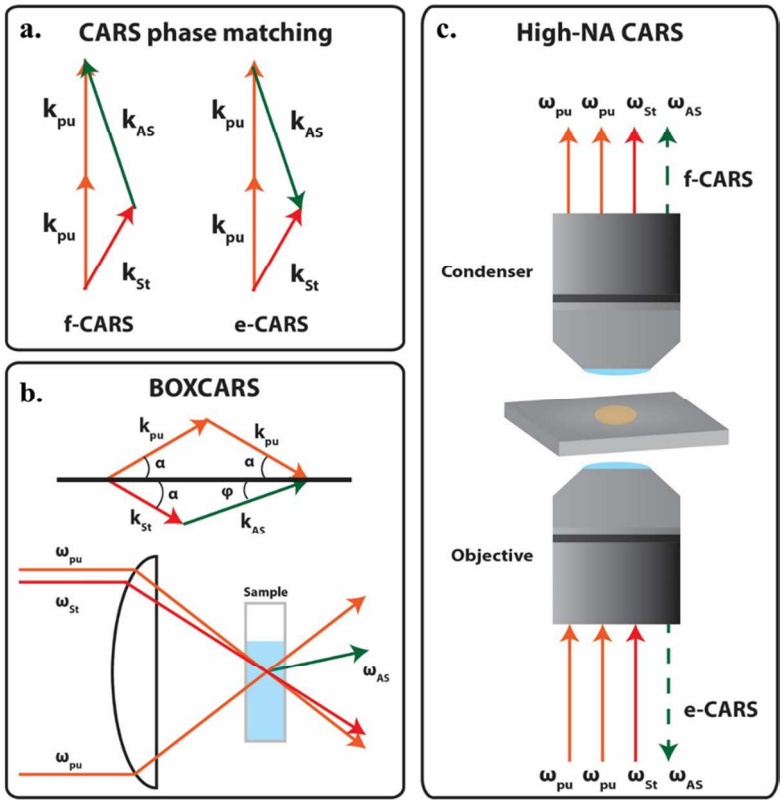

Fig. 6: a) General phase matching (k) conditions of both forward CARS (f-CARS) and epidirectional CARS (e-CARS) for the pump (pu), Stokes (St), and anti-Stokes fields (AS) for CARS signal generation. b) f-CARS BOXCAR phase matching experimental geometry showing frequencies (ω). c) High numerical aperture (high-NA) phase matching experimental geometry using microscope optics.

Using a combination of improved CARS experimental techniques and plasmonic substrate synthesis, surface-enhanced coherent anti-Stokes Raman scattering (SECARS) has developed into one of the most promising fields of plasmonically-enhanced ultrafast Raman spectroscopy.[156] In this section we discuss the initial fundamental experimental studies of SECARS, theory of SECARS to better understand experimental conditions and enhancement factors, and the most recent developments in SECARS: single molecule and time-resolved studies.

3.3.2 Fundamental studies of plasmonic enhancement in SECARS

The first report of SECARS came from the Shen group in 1979.[157] Like other early studies of CARS,[147] Shen focused on a system of benzene adsorbed on silver surfaces. They obtained a CARS spectrum of the 992 cm^{-1} mode of neat benzene as a control experiment while measuring the SECARS spectrum of benzene on a silver surface in parallel. By exciting the surface plasmons in the silver film, they observed a plasmonically-enhanced CARS signal. Even in this early report, the power of SECARS was suggested to probe sub-monolayer assemblies of molecules on surfaces.[157] As we will see in Section

3.3.4, this early prediction was recently verified and extended beyond sub-monolayer coverage to the single molecule limit.[9, 10, 158] After this initial study, Liang et al. continued work of SECARS by studying mixtures of benzene, N,N'-dimethylformamide, toluene, and chlorobenzene in Ag colloidal solutions.[159] Liang et al. used a Q-switched nanosecond Nd:YAG laser to pump two dye lasers for the pump and Stokes pulses. Using the tunability of the dye lasers, they tracked the EF of the 992 cm^{-1} mode of benzene as a function of pulse wavelength and saw strong pump wavelength dependence. As the pump was tuned from 458 nm to 521 nm, an optimum enhancement was observed near 500 nm; likely close to the aggregate Ag colloidal LSPR.[160] This highlights the importance of substrate characterization in modern ultrafast SERS techniques, so as to tune pulses for ideal enhancement. While the authors observed SECARS from a variety of analytes, the EFs reported were only on the order of 10^2 over CARS.

To simplify the phase-matching requirements in SECARS, the Kawata group applied the high-NA CARS microscopy technique[149, 161] to perform SECARS microspectroscopy.[162] The experimental setup involved two synchronously pumped Ti:Sapphire oscillators that were collinearly focused into an objective, and the SECARS signal was recorded from adenine reporter molecules on single Au particle aggregates. The researchers suggested SECARS microspectroscopy could be used to image localized hot spots as only few nanoparticle aggregates with presumably highly enhancing hot spots[163] gave the overwhelmingly largest CARS signal. However, similar to previous SECARS attempts, the EF observed was only 2-6 × 10^3 over CARS, far lower than the typical 10^8 enhancements seen in SMSERS.[4]

The Popp group was the first to apply the methods of SECARS to biological applications.[164] Schlücker et al. employed SECARS to demonstrate a new method of immunohistochemistry coupled with microscopy to improve optical contrast in biological specimens. Using alloyed plasmonic Au/Ag nanoshells, the authors grew self-assembled monolayers of Raman reporter molecules (DTNB) on the nanoparticle surface and then incubated the substrates in a solution of p63 antibodies (IgG). The completed nanoprobes were then incubated in slices of prostate tissue. They used SECARS microscopy to observe high contrast images of the p-63 antibody tagged nanoprobes in the prostate tissue conjugated with p63-(+) basal epithelium and p63-(-) secretory epithelium by tuning the CARS pulse sequence spectrally to be in resonance with a DTNB vibrational mode. This paper clearly suggests the future use of SECARS for its sensitive vibrational imaging and the possible rapid detection of target molecules in complex biological specimens.

In 2009 the Turner group plasmonically enhanced SHG and CARS signals using self-assembled gold nanoparticle substrates.[165] Addison et al. deposited layers of 14-nm gold spheres on a glass substrate using dithiol linker molecules to connect nanoparticles in the presence of an oxazine 720 analyte. SECARS signal of oxazine 720 was recorded at 1600 and 3000 cm^{-1} to monitor the plasmonic enhancement of the CARS signal with a maximum enhancement of 10 over CARS.[165] Steuwe et al., also explored new plasmonic substrate designs by recording SECARS of benzenethiol on in-house produced substrates and a commercial plasmonic substrate, Klarite.[166] SECARS showed excellent imaging capabilities, reproducing the SEM-determined structure of Klarite by SECARS imaging of a single vibrational mode in benzenethiol. The enhancements for the in-house fabricated

substrates reported were on the range of 10^9-10^{10} over NRS of benzenethiol. Therefore these were the first highly enhancing SECARS substrates as previous studies consistently showed EF's of 10^1-10^3.[159, 162, 165] With the enhancements observed in this study, the authors suggest that this approach may allow for better photostability in single molecule spectroscopy.

The fundamental studies of SECARS done since the first work in the Shen group[157] have focused on observing various organic analytes in colloidal solutions,[159] demonstrating biological imaging,[164] new experimental CARS microscopy techniques,[162] and improving substrate selection in SECARS.[164-166] The understanding these initial works provided of optimal experimental design choices for both laser and substrate parameters in SECARS was critical to the later successes of the SECARS field that we will discuss in the following sections.

3.3.3 Theoretical studies of SECARS

Based on the results of the Shen group,[157] the Kerker group developed an early theoretical framework for the plasmonic enhancement in SECARS.[167] Chew et al. considered a system of benzene on Ag nanospheres in solution similar to the system probed by Shen.[157] While the theoretical system Chew et al. described didn't include the 'hot spots' that are thought to be the dominant source of highly enhancing Raman signal,[163] they predicted enhancement factors up to 10^{21} over CARS. This early recognition that the multiple coupled fields in CARS all can be enhanced by the plasmon oscillation of the nanoparticle gave predictions based on all fields being resonant with the plasmonic substrate. However, with more realistic experimental considerations including phase-matching and solid angle signal collection, still with all optical fields being plasmonically resonant, the generally accepted enhancement factors of SECARS have been lowered.[10, 168-170]

A significant improvement on SECARS theory came from the Aspuru-Guzik group who studied issues associated with modeling SECARS spectra as well as why the originally predicted high EFs[167] have yet to be observed experimentally.[168] One of the difficulties in modeling SECARS spectra is expressing the resonant and nonresonant CARS susceptibilities in simple forms. Significant progress was made on the relevant susceptibilities for SECARS by reducing $\chi^{(3)}$ to a product of dynamic $\chi^{(1)}$ susceptibilities.[171] Using the product of linear susceptibilities, they modeled a few molecular systems including pyridine on Ag cluster complexes. From their calculations they showed enhancement factors between zero and 700 depending on surface adsorption effects in the HOMO-LUMO gap of the pyridine-Ag complex. In addition the authors discuss some of the issues that may contribute to the lack of large EFs; primarily the idea of phase-matching near metal surfaces, background signals from other $\chi^{(3)}$ processes, and vibrational dephasing. While spontaneous Raman scattering experiments have weak dependence on vibrational dephasing, the SECARS spectra will be affected due to the resonant CARS wavepacket needing to pass through a vibrational coherence and interact with an optical field again to contribute signal. Hence, the understanding of the observed plasmonic enhancement in coherent Raman techniques goes beyond the simple optical field plasmonic enhancement in SERS.[168] To understand the plasmonic enhancement of SECARS, or any

other surface-enhanced coherent Raman scattering experiment, one must take full consideration of both the coherent scattering process and the plasmonic field enhancements.

Continuing to consider the phase-matching effects near metal surfaces that were proposed by the Aspuru-Guzik group,[168] the Scully group provided a theoretical and experimental study that attempted to address the lack of high EF's in ensemble colloidal SECARS measurements.[169] The researchers postulated that the weaker-than-predicted EFs in SECARS arise from the phase mismatch between the optical fields present in the coherent scattering process of SECARS and the phase of the plasmonically-enhancing field. Using SECARS experimental data of pyridine on Au nanoparticle aggregates, they provided simulations that reproduced the observed varying spectral line shapes (positive, negative, and dispersive Lorentzian) that varied with respect to the phase of the exciting fields with the plasmon resonance. To further understand the spectral line shapes indicative of molecular resonance effects,[172] the Scully group focused on a pyridazine –gold nanoparticle system.[170] In their study, the line shapes could be explained by arguing that the spectra observed are dependent on two separate pyridazine-gold complexes that vary in the number of gold atoms over which the pyridazine frontier orbitals are delocalized. The combined work of the Scully group has established the need for considering different interference effects of the excitation and signal fields and the molecule-nanoparticle system at an atomistic level for explaining SECARS spectra.

Theory of SECARS has evolved since the early work of the Kerker group.[167] The SECARS theoretical community has understood that the observed plasmonic enhancement factors in coherent Raman techniques aren't as simple as plasmonically enhancing the optical excitation fields. To fully understand surface-enhanced coherent Raman techniques, a combination of phase-matching,[168-170] vibrational dephasing,[168] signal interference,[169, 170] and plasmonic enhancement[167-170] are required. This work not only informs recent experimental progress in SECARS but also highlights a number of important points to be considered when studying the enhancement mechanisms of other ultrafast SERS techniques.

3.3.4 Experimental progress in single molecule and time resolved SECARS

Two of the more exciting developments in the SECARS field are the recent proof of single molecule sensitivity and observation of time-dependent phenomenon. Building on the earlier works discussed, these achievements open the door to use SECARS to study ultrafast molecular plasmonics.

Using high-NA SECARS microspectroscopy, the Berlin group had the first single molecule SECARS claim.[158] The system was deoxyguanosine monophosphate (dGMP) in a silver colloidal solution. The authors used two synchronized picosecond Ti:Sapphire oscillators collinearly focused into a microscope objective and collected epi-direction SECARS signal. Using this technique, a single vibrational mode of dGMP was observed at concentration levels consistent with single molecule[3, 4] studies. However, no isotopologue, bianalyte, or large statistical measurements were performed to provide definitive proof for their single molecule claim.

A bianalyte[3] single molecule SECARS study was done by the Halas group in 2014.[10] Zhang et al. used SECARS microspectroscopy to obtain spectra of para-mercaptoaniline (p-MA) and adenine on lithographically prepared Au quadrumers (see Figure 7a). The plasmonic substrate was optimized for minimizing losses of the pump wavelength and maximizing the scattering of anti-Stokes emission, as illustrated in Figure 7b and c. The quadrumer substrates were designed with a subradiant mode near the pump and broad superradiant modes in the Stokes and anti-Stokes field regions. Experimentally, a femtosecond 76 MHz Ti:Sapphire oscillator was used to generate the 800 nm pump and drive continuum generation in a photonic crystal fiber for the Stokes pulse. These pulses were then focused into a microscope and scanned across an array of the lithographically prepared quadrumers to collect the spectrally resolved SECARS signal. With enhancement factors of 10^{11} over spontaneous Raman scattering, the authors measured spectra of each of the two analytes as well as mixed events with signatures from both (see Figure 7d). They verified single molecule detection by building a histogram representative of single molecule events by the bianalyte approach.[10] With single molecule sensitivity, SECARS can now be applied to an even wider range of potential applications.

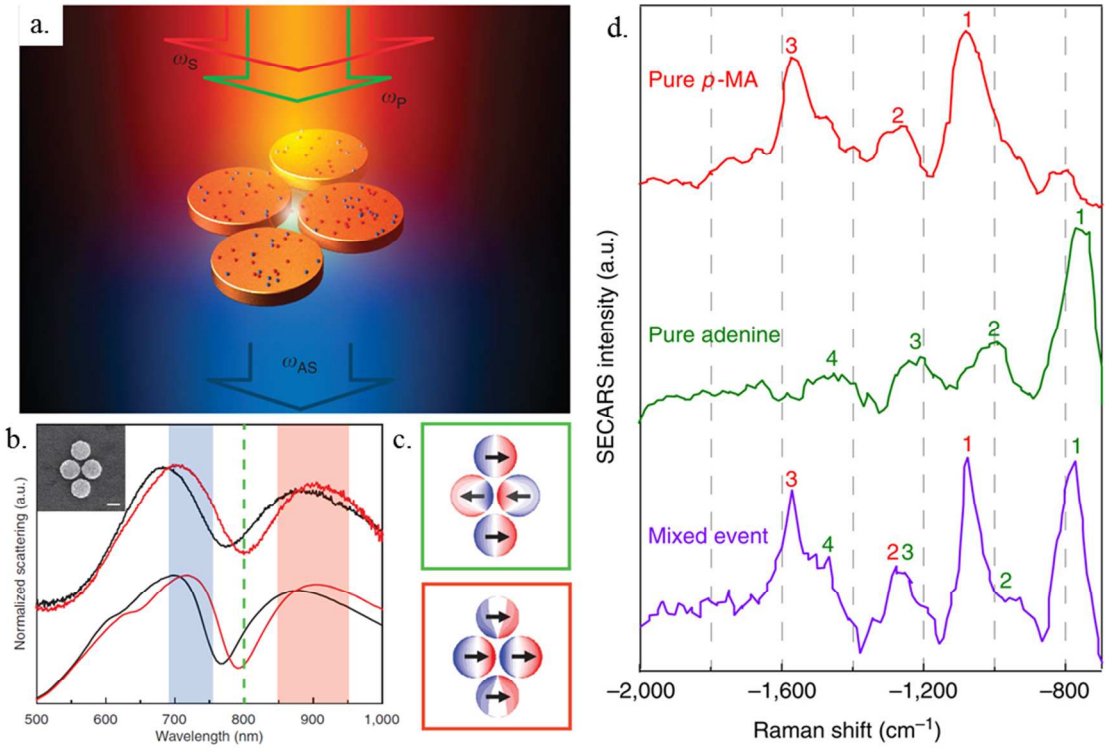

Figure 7. a) Schematic of quadrumer substrate structure used in SECARS study. b) LSPR of quadrumer substrates where the green dashed line indicates the pump pulse, red shaded region indicates the bandwidth of the Stokes pulse, and the blue shaded region indicates the anti-Stokes signal region. c) Diagram of the subradiant (top) and superradiant (bottom) hybrid plasmon modes. d) Experimental data of single molecule SECARS. The top two traces show single analyte behavior while the bottom trace is an example of a mixed event. Adapted by permission from Macmillan Publishers Ltd: *Nature Communications* reference [10], copyright 2014.

The second important development in the field of SECARS is the study of ultrafast dynamics. Introduction of time resolution to SECARS came in 2012 from the Scully group.[173] The first report of TR-SECARS analyzed pyridine-water complexes on gold colloids. In particular, the work was significant as it showed the use of pulse-shaping and timing delays to suppress the nonresonant background signal from the plasmonic particles. By temporally delaying a sinc-shaped probe pulse,[174] the authors observed the ring breathing mode of a pyridine-water complex and vibrational dephasing times greater than ten picoseconds for pyridine near nanoparticles. This first work on TR-SECARS reported an enhancement factor of 10^7 for TR-SECARS compared to bulk CARS.

Bringing together single molecule spectroscopy with time resolution, the Apkarian group performed the first single molecule time-resolved SECARS study.[9] Using silica-coated Au nanoparticle aggregates with *trans*-1,2-bis(4-pyridyl)-ethylene (BPE) as a reporter molecule, Yampolsky et al. performed TR-SECARS and observed quantum beating of vibrational modes indicative of a single molecule. This beating behavior was verified by simulated probability distribution functions of the noise in early time responses seen in Figure 8c. At a repetition rate of 80 MHz, the pump and probe pulses at 714 nm and the Stokes pulse at 809 nm drove the oscillation of the strong 1640 cm^{-1} vibrational mode in BPE seen in Figure 8b. The time resolution of this experiment allowed for monitoring the vibrational beating of between the 1647 and 1612 cm^{-1} modes over long periods of time relative to plasmon dephasing processes. In the bulk SECARS experiment, the beating dies in approximately one picosecond, however in the single aggregate experiment, the beating persists for the entire ten picosecond experimental window, seen in Figure 8c. This suggests that the vibrational dephasing on the single aggregate level is not strongly perturbed by the near-field LSPR. This illustrates the potential of single molecule photoexcited studies near plasmonic surfaces.

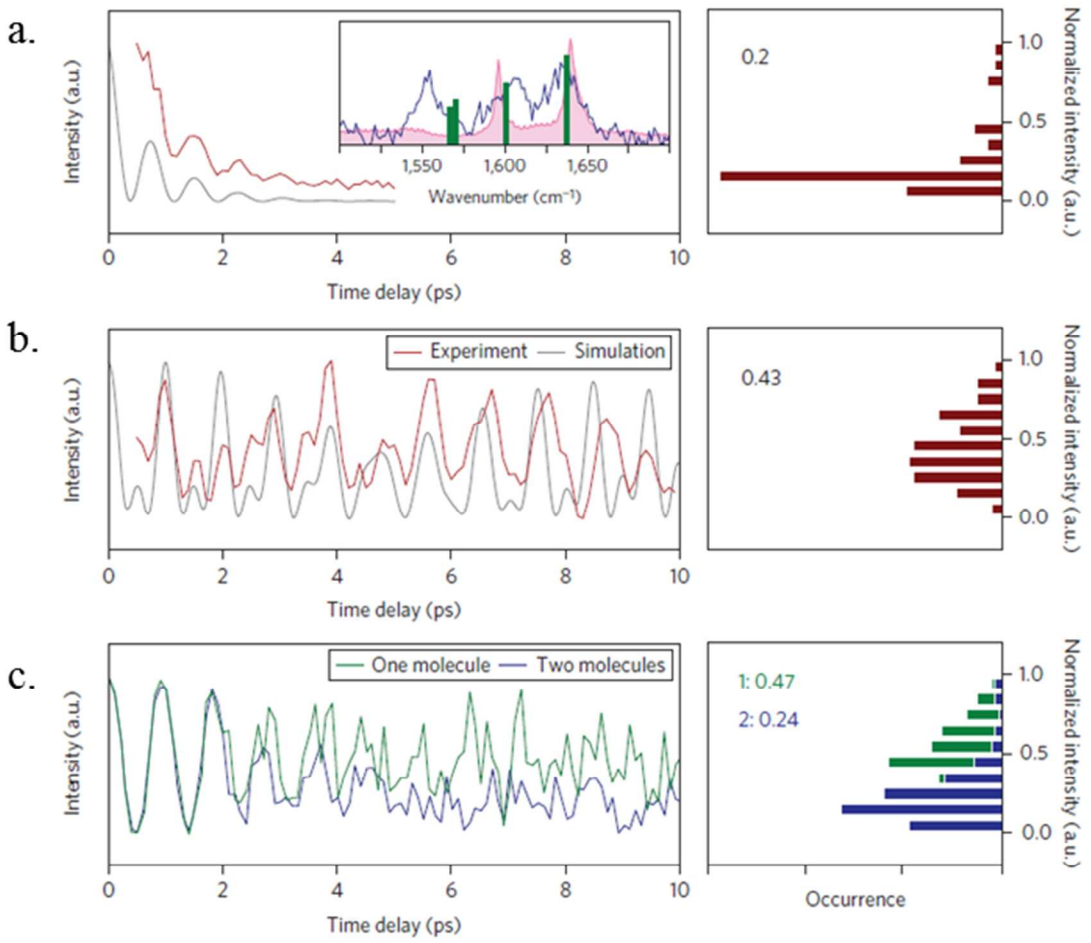

Figure 8. a) (Left) Bulk TR-CARS spectrum of BPE (brown curve) with the windowed Fourier transform of the bulk normal Raman spectrum (grey curve). (Left, inset) bulk normal Raman spectrum of BPE (pink curve), transient SERS spectrum (blue curve) of nanoparticle substrate that TR-SECARS transient in (b) is displayed. (Right) probability distribution function (PDF) and first moment derived from transient SECARS spectrum on left. b) (Left) Experimental transient TR-SECARS of single particle that shows distinct long lived quantum beating of the vibrational modes indicated in the green stick spectrum of the inset of (a). (Right) PDF and first moment showing the single molecule behavior indicated by moment of ~0.5. c) (Left) Simulations of one (green curve) and two (blue curve) molecule quantum beating at long transient times. (Right) PDFs and first moments for simulated one and two molecule quantum beating data showing the expected moment of ~0.5 for a single molecule. Adapted by permission from Macmillan Publishers Ltd: *Nature Photonics* reference [9], copyright 2014.

SECARS has grown considerably from the initial report of enhanced benzene CARS spectra on a silver film.[157] The field has now proven single molecule sensitivity,[9, 10] ultrafast time resolution,[9, 173] and biological relevancy.[164] In addition, theoretical studies were developed[10, 168-170] to explain the observed EFs and line shapes. SECARS is one of the more widely used ultrafast SERS techniques. Thus as one of the most well-developed tools to study coupled molecule-plasmon systems, SECARS will continue to grow as a method

of single molecule, time-resolved spectroscopy to track chemistry on ultrafast time scales near plasmonic surfaces.

3.4 Surface-enhanced Femtosecond Stimulated Raman Spectroscopy (SEFSRS)

Another recent successful combination of ultrafast nonlinear Raman spectroscopy with SERS was the first demonstration of surface-enhanced femtosecond stimulated Raman spectroscopy (SEFSRS) in the Van Duyne group.[175]

3.4.1 FSRS and early attempts to incorporate plasmonic substrates

Femtosecond stimulated Raman spectroscopy (FSRS) is a relatively new time-resolved technique which enables the acquisition of vibrational spectra with ultrafast time resolution.[176-178] FSRS is a nonlinear Raman spectroscopy that utilizes stimulated Raman scattering to overcome fluorescence and the inherently low Raman cross section of most molecules, as discussed in Section 2.2. This technique allows for the one-shot acquisition of a broad, high-resolution Raman spectrum at varying time delays after photoexcitation for both high spectral (typically 5-20 cm^{-1}) and temporal (10-100 fs) resolution. Ground state FSRS spectra are obtained when a narrow bandwidth picosecond Raman pump pulse and a broadband femtosecond probe pulse simultaneously interrogate a Raman active analyte. As depicted in Figure 5, the probe and Raman pump pulses first interact with a molecule, establishing a vibrational coherence. A second interaction with the pump pulse then leads to the stimulated emission of a Stokes-shifted photon when energy is transferred from the Raman pump to the stimulating probe at the frequency shifts of Raman-active modes in the interrogated molecules. This leads to sharp bands which are Stokes-shifted from the narrowband Raman pump on top of the broad probe spectrum (see Figure 9). A FSRS spectrum is produced by dividing Raman pump "off" spectra from Raman pump "on" to give Raman gain as a function of Raman shift. This implementation provides information on ground state vibrational frequencies, and with a stimulated Raman setup, all Raman information is emitted in a heterodyned fashion, enabling easy setup and data acquisition. To study molecular dynamics, FSRS utilizes a femtosecond actinic pump pulse to first photoexcite a molecular system before the probe and Raman pump pulses interact with an analyte. The structural evolution of the excited state is subsequently probed at various time points during a reaction. The evolution of the vibrational spectrum during a chemical transformation provides key structural data on the reaction mechanism.

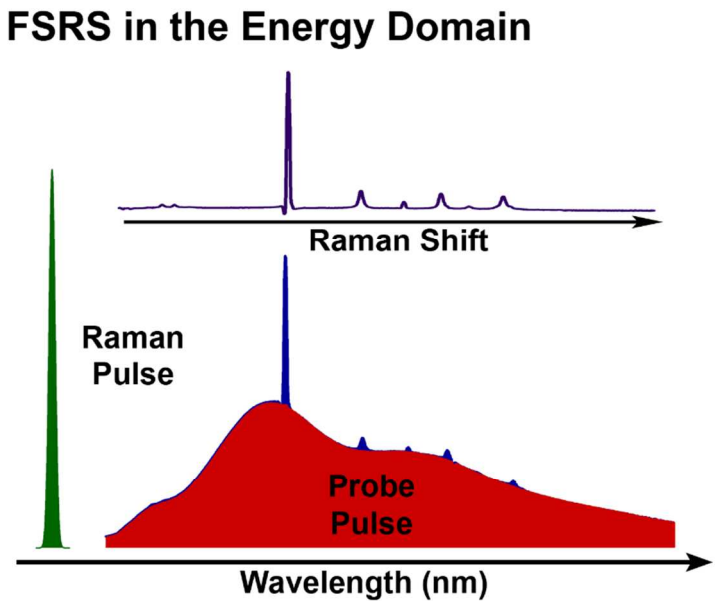

Figure 9. Representation of the pulses used in FSRS. The energy domain demonstrates how a broadband probe just red shifted from a narrowband Raman pump pulse interrogates a broad Stokes shifted region of a Raman spectrum. A Raman spectrum is obtained when the probe pulse spectrum is divided out, as seen above the probe spectrum. Figure reproduced from reference [178]. Copyright, 2011 by WILEY-VCH Verlag GmbH & Co. KGaA, Weinheim.

This novel approach has been used to reveal study excited state vibrational dynamics in a number of biological systems,[179-181] photovoltaic materials,[182-186] and more. For example, FSRS was used to investigate important structural changes that control ultrafast processes including proton transfer in green fluorescent protein[22] and state changes during ultrafast intersystem crossing in the dye tris(bipyridine)ruthenium(II) ($Ru(bpy)_3^{2+}$).[187]

Despite its advantages, FSRS is typically limited to studying ensemble dynamics of highly concentrated samples with relatively large Raman cross sections. This can require large volumes of sample and necessitates that FSRS samples will have some form of heterogeneity. Combining SERS with FSRS could overcome these limitations by amplifying fundamentally weak Raman scattering from a small number of molecules near nanostructured SERS hotspots. Early attempts by Ploetz et al. were made to combine FSRS and SERS, looking for enhancement of organic monolayers on gold and silver nanoshells.[188] With 75 nJ/pulse of Raman pump power at a 1 kHz repetition rate and a plasmonic substrate in resonance with the Raman pump, they were unable to observe surface-enhanced FSRS signals. When the high fields from these focused ultrafast pulses are amplified and concentrated by plasmonic materials, the field strengths rapidly approach the dielectric breakdown limit for organic molecules. Thus attempts to obtain SEFSRS data from typical 1 kHz amplified laser systems have failed at this point. This highlights one of the major difficulties with these surface-enhanced ultrafast techniques; it is necessary to consider both peak power and electromagnetic enhancement factors when performing these experiments so as to not damage both the plasmonic structures and the molecules of interest.

3.4.2 Development of SEFSRS

The Van Duyne group was able to successfully combine SERS and FSRS in 2011 using a 100 kHz repetition rate laser system with pulse energies high enough for signal generation, but low peak powers to avoid damage to the substrates.[175] Frontiera et al. demonstrated SEFSRS on aggregated gold colloids with adsorbed reporter molecules and an encapsulating silica shell (see Figure 10a), which were later used in TR-SECARS experiments[9] as well. This proof-of-principle paper presented ground-state SEFSRS spectra with characteristic Fano-like lineshapes (see figure 10b). The authors conservatively estimated time- and ensemble- averaged enhancement factors for SEFSRS to be 10^4-10^6, however this estimated EF was limited by degradation. The dependence of SEFSRS gain on Raman pump power was shown to be linear only in extremely low power regimes, after which the signal saturates. Additionally, the signal decreased on the minute timescale, and the localized surface plasmon resonance saw a loss in the NIR longitudinal resonance after prolonged irradiation with the high-powered Raman pump pulse. These results indicated damage occurred in these original SEFSRS experiments, most likely to the plasmonic aggregates since no changes were observed in the Raman spectrum to indicate photodamage to the molecular analyte.

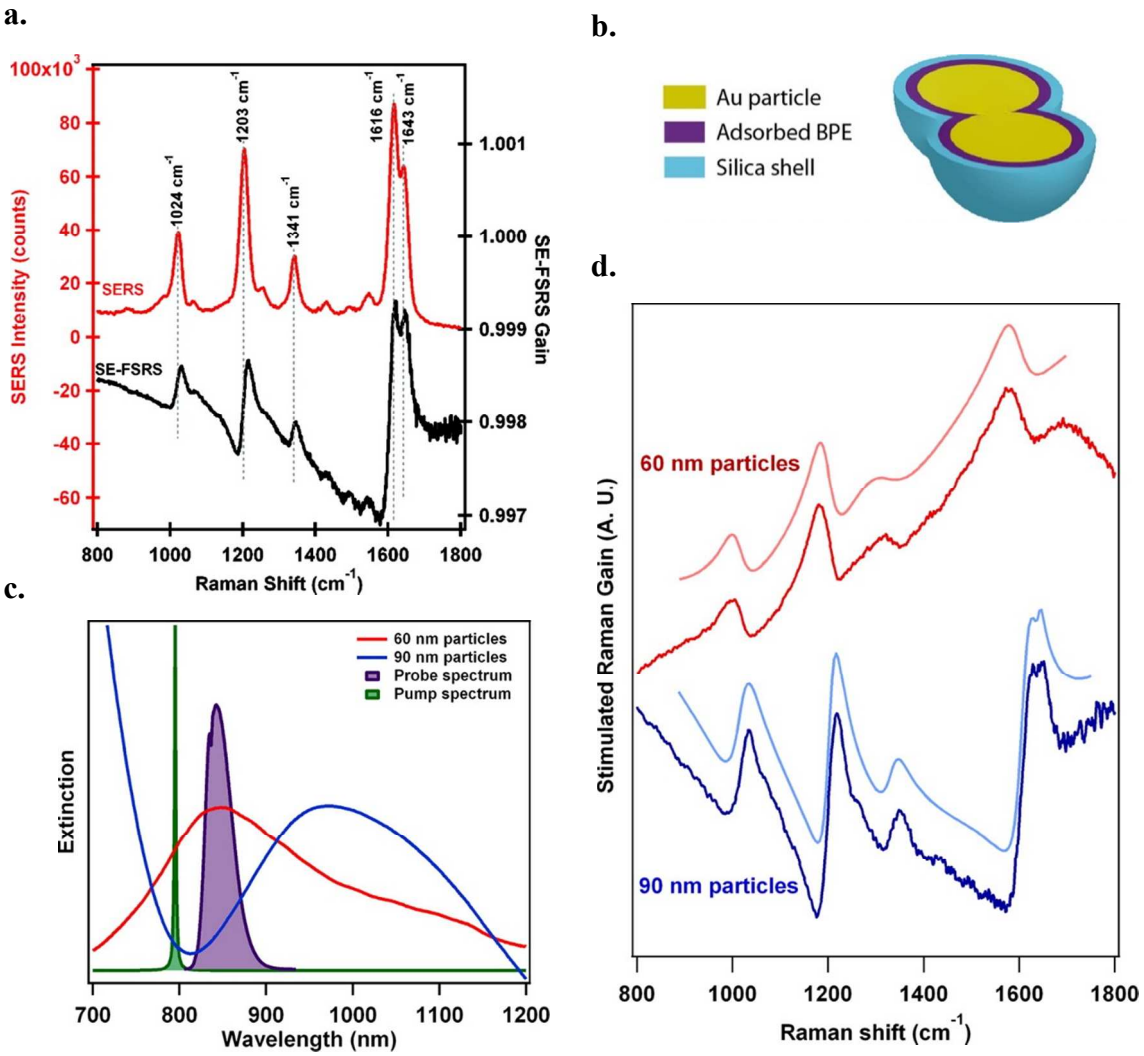

Figure 10. a) SEFSRS spectrum (black) and picosecond spontaneous SERS spectrum (red) of BPE , illustrating the dispersive lineshapes and high signal-to-noise after under 10 minutes of averaging at 2.0 nJ/pulse Raman pump energy and 100 pJ/pulse probe energy. From reference [175]. Copyright 2011 American Chemical Society. b) The substrate used for the first SEFSRS experiments was a colloidal solution of gold 90-nm diameter nanospheres which are aggregated, coated in adsorbed BPE analyte molecules, and then protected by a layer of silica. This representation shows a dimer particle, with a hotspot between the particles, which will provide the highest enhancement. The solution also contains monomer particles without hotspots and larger aggregates. c) Spectra of the pump and probe pulses, in green and purple respectively, are compared to the plasmon resonance energies of the aggregated 90-nm and 60-nm Au spheres. Notably, the 60-nm spheres have an LSPR that overlaps with the probe spectrum, while the 90-nm sample has an LSPR maximum to the red of the probe. d) The SEFSRS spectra of the 60-nm (dark red) and 90-nm (dark blue) samples are plotted with their Fano fits offset above. From reference [12]. Copyright 2012 American Chemical Society.

The following year the Van Duyne group followed up with a more in-depth investigation into the observed Fano-like resonances arising from these colloidal nanoparticle-molecular systems.[12] By varying the size of the nanoparticle substrates, Frontiera et al. changed the energy of the plasmon resonances of the substrate with respect to the wavelengths of the Raman pump and stimulating probe pulses (see Figure 10c). This change in plasmon resonance energy resulted in a change in the phase of the dispersion of the observed peaks, which were fit to a Fano function (see Figure 10d). This suggests that the Fano-like lineshapes arise from an interaction of the narrow molecular vibrational coherence and the broad plasmon resonance of the colloidal nanoparticles. The authors then studied the effect of this coupling on the vibrational coherence lifetime of the analyte molecules. One concern in using an ultrafast Raman technique such as FSRS in conjunction with SERS is that the vibrational coherences required to generate signal may be quenched when molecules are placed in close proximity to plasmonic surfaces. SERS measurements of highly fluorescent dye molecules have proven that molecular excited electronic states are rapidly quenched by the presence of nearby plasmons, primarily through a resonant energy transfer mechanism. Although vibrational coherences are much lower in energy than the visible and near infrared plasmons, before this SEFSRS work, it was largely unknown what the behavior and lifetime of the vibrational coherences would be. These long-lived coherences were also observed in time-resolved SECARS measurements by the Scully group,[173] as previously discussed. Using SEFSRS, the Van Duyne group showed that this lifetime is not significantly shortened, despite the proximity of the metal nanoparticle surface and the observed plasmon-molecule coupling. These results pave the way for SEFSRS to be used to study ultrafast dynamics in plasmonically-enhanced molecular systems. If SEFSRS could be coupled with a microscope, similar to the SECARS experiments by the Apakarian and Halas groups,[9, 10] and brought close to the single molecule detection level it could be a powerful tool for the study of reaction dynamics near metal surfaces.

3.5 Ultrafast tip-enhanced Raman spectroscopies

3.5.1 Tip-enhanced Raman scattering

A major goal of the ultrafast SERS field is to understand how molecule-plasmon coupled systems interact on the nanoscale. One approach that has the potential to combine single molecule sensitivity with both high spatial and temporal resolution is ultrafast tip-enhanced Raman spectroscopy (TERS). Inspired by the amplification of Raman signals observed in SERS, several tip-enhanced vibrational spectroscopies have been developed over the past 15 years.[5, 189-192] These approaches vary, but in general utilized scanning probe microscopy (SPM) with metallic nanoprobe tip which can characterize nano- and sometimes atomic-scale surfaces while plasmonically enhancing vibrational signatures from a small subset of molecules under tip (see Figure 11).

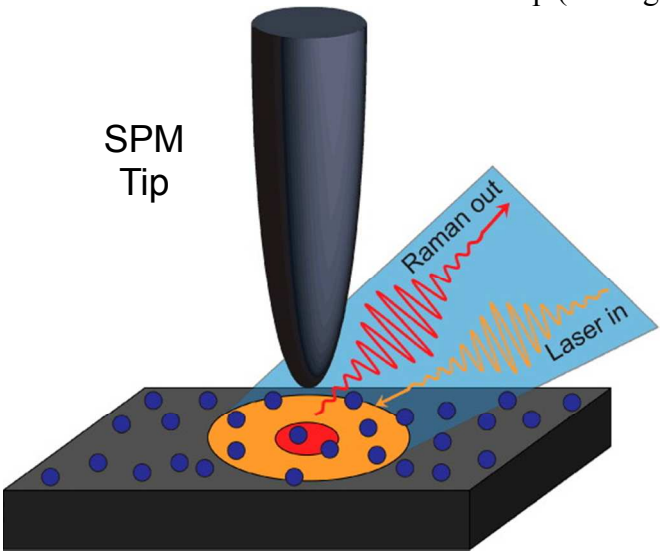

Figure 11. Schematic for tip-enhanced vibrational spectroscopies: a plasmonic SPM tip brought near a substrate with a molecular adsorbate (represented by blue dots). Note that in the wide field of laser irradiation (yellow circle), the enhanced scattering occurs selectively under the tip (red circle). Reprinted and adapted with permission from reference [193]. Copyright 2014 American Chemical Society.

Tip-enhanced Raman spectroscopy (TERS)[194-196] is a highly sensitive technique that can provide surface characterization with the atomic-resolution expected from scanning probe techniques along with chemical information from vibrational Raman spectra of samples as small as single molecules.[5, 8, 197] TERS uses plasmonic probes, usually silver or gold tips that are to enhance Raman scattering from a small domain underneath the probe apex. This allows for sub-diffraction limited lateral resolution, as the signal is selectively enhanced not in the full area of the laser focal spot but instead under and around the tip apex.[198] The substrates beneath the tip can be plasmonic or non-plasmonic in nature, the first case providing additional enhancements from the so-called 'gap mode' plasmon between the tip and the surface. The scanning probes can be standard scanning tunneling microscopy (STM) or atomic force microscopy (AFM) probes that are nanoscale gold and silver tips, or standard probes coated in a plasmonic layer.[195] TER imaging has been used to characterize adsorbates on a surface with nanometer resolution and sub-single molecule resolution.[8] It is therefore a promising candidate for combination with ultrafast techniques as the field works towards combining single molecule sensitivity with femtosecond temporal resolution.

Though promising, ultrafast TERS and other ultrafast tip-enhanced spectroscopies have been slow to develop as they involve complex experimental set-ups as well as potential molecular damage by highly localized plasmonically enhanced electric fields in the tip-sample junction. However, both spontaneous and stimulated ultrafast TERS experiments have been successful, and recent results highlight the possibly of time-resolved TERS. Here, we review these recent advances.

3.5.2 Tip-enhanced CARS

One of the earliest and most-developed application of ultrafast TERS has been tip-enhanced coherent anti-Stokes Raman spectroscopy (TECARS). The Kawata group first applied their SECARS microscopy studies to TECARS in 2004. First, they reported TE-CAR images of adenine molecules in DNA clusters, as shown in Figure 12.[199, 200] They were able to couple 5 ps pulses with the plasmonic tip with average powers of approximately 30 -100 μW at a 800 kHz repetition rate The authors reported spatial resolution beyond the diffraction limit of light due to the localization of the electric field enhancement underneath the metallic nanoprobe. Using silver-coated AFM cantilever, they imaged nanoclusters of DNA fragments on resonance with the diazole adenine ring-breathing vibrational mode with an estimated enhancement factor of ~100 over CARS (see Figure 12). The Kawata acquired TE-CAR images and correlated AFM images of single-wall carbon nanotubes using gold-coated cantilevers.[201] Recently, Kawata and coworkers, optimized the technique using a broadband Stokes pulse to quickly measure multiplex Raman spectra without scanning wavelengths.[11] The authors demonstrated tip-enhanced broadband coherent anti-Stokes Raman (TE-BB-CAR) spectra and images of semiconducting carbon nanotubes. They obtained multiplexed TE-BB-CAR images from 900 to 2200 cm^{-1} with a spatial resolution of 60 nm by combining a supercontinuum from a photonic crystal fiber and a gold-coated glass fiber tip on a tuning-fork based shear-force microscope setup. Though their enhancement factors were small (less than one order of magnitude), the authors were able to demonstrate that the TE-BB-CARS signal provided enough positive contrast for high-resolution imaging by combining ultrafast pulses with plasmonic probes. They also observed a longer decay (~3 ps) of the G-band signal from the S-CNTs in the near field compared to the far field (~1.5 ps), possibly due to an Auger process induced at unusually high intensities beneath the tip. This is the first reported study of ultrafast dynamics using time-resolved TECARS. Combining the ability to study dynamics with the ability to image material with ultrafast pulses and high sensitivity, TECARS has opened the door to plasmon-mediated dynamics in a variety of materials.

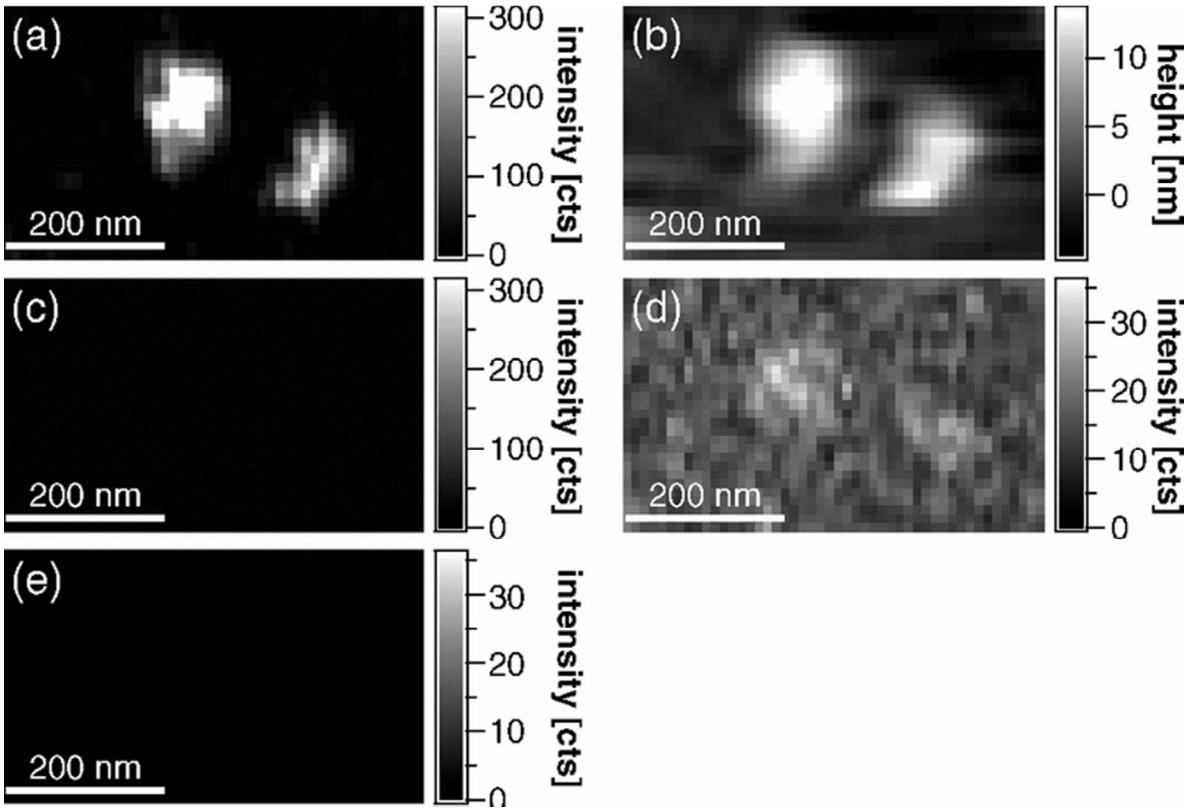

Figure 12. Tip-enhanced CARS images of DNA clusters. A TECARS image (a) on-resonance with the ring-breathing mode of diazole in adenine molecules (1337 rel cm^{-1}) and the corresponding topographic AFM image (b) show excellent agreement. The TECARS image (c) at an off-resonant frequency (1278 rel cm^{-1}) illustrates the success of the TECARS experiment to image selective modes (also shown in (d) with a different greyscale). And the unenhanced CAR image (e) taken without a plasmonic probe illustrates the plasmonic enhancements of approximately 100. Reprinted and adapted with permission from reference [199]. Copyright 2004 by the American Physical Society.

3.5.3 Picosecond TERS and challenges combining TERS with ultrafast pulses

Despite these advances in ultrafast TERS, there are inherent difficulties that arise from the high pulse energies and concentrated fields used in these experiments, just as in the SERS experiments. In 2013, Klingsporn et al. explored the limitations of ultrafast TERS with respect to signal loss due to damaging the adsorbate and/or the plasmonic tip.[193] The authors compared the ambient STM-TERS spectra of resonant dyes using picosecond and cw excitation. They found that the tip was not damaged by the ultrafast excitation pulses, but that the ps-TERS signal decayed in tens of seconds while the cw-TERS spectra showed no such decay. Figure 13 illustrates the decay of the ps TERS signal as a function of time, fit to both first order kinetics ($e^{-k/\tau}$) to model reactive decay chemistry or photothermal desorption, as well as inverse square root ($t^{-1/2}$) to model surface diffusion. Diffusion is unlikely because the malachite green isothiocyanate (MGITC) molecules were covalently attached to the surface. The authors concluded the observed decay is due to either the

presence of H_2O and O_2 leading to reactive decay or desorption of the molecules due to plasmonic and photothermal heating in the hotspots under the tip. Either of these mechanisms could be alleviated in an ultra-high vacuum (UHV) environment. Therefore, the following year Pozzi et al. performed similar experiments in UHV in order to better understand the observed ps-TERS decay mechanism.[202] They found that the TERS response of Rhodamine 6G (R6G) and MGITC dye molecules did not undergo irreversible degradation in high vacuum. The authors found that both diffusion and reaction of the analyte molecules led to loss of TERS signal from pulsed excitation, but that the lack of oxygen limited decay of the TERS signal. They concluded that reactive decay dominated the signal loss from a chemisorbed species (MGITC), while diffusion dominated the loss of signal from a physisorbed analyte (R6G). This work provides important parameters for future ultrafast TERS experiments, especially as the field works towards studying ultrafast dynamics with high sensitivity. It suggests that ultrafast TERS experiments that take advantage of high enhancement factors and resonance enhancements may require measures to mitigate signal loss.

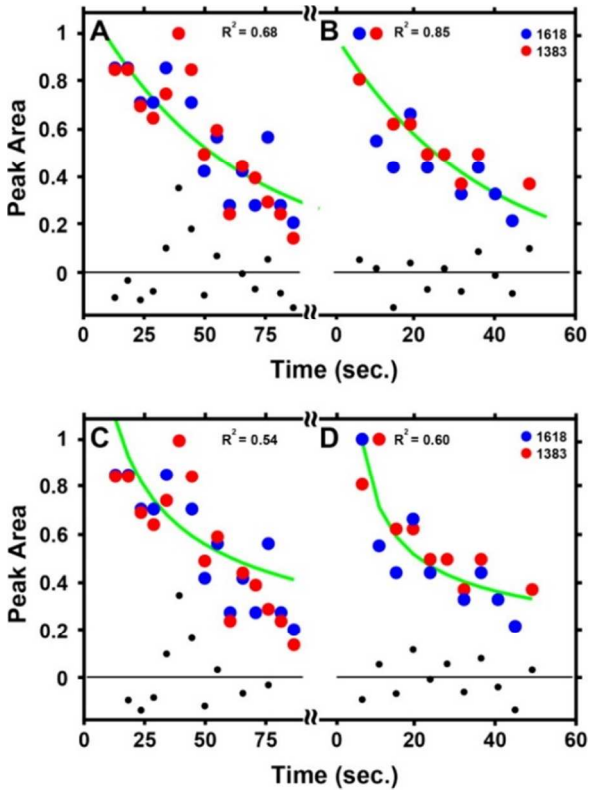

Figure 13. Decay of the ps TERS integrated intensities at 1618 (blue) and 1383 (red) relative wavenumbers of MGITC at two different spots within the laser focus, as noted by the break in the x-axis. The top data (a,b) is fit (green) to exponential first-order kintetics ($e^{-k/\tau}$) while the same data below (c,d) are fit (green) as an inverse square root ($t^{-1/2}$) for modelling of surface diffusion. Residuals are plotted below the fits. The R^2 values indicate the signal is more likely from photothermal desorption or reactive decay chemistry, as fit by first order kinetics, as opposed to diffusion. Reprinted with permission from reference [193]. Copyright 2014 American Chemical Society.

While the majority of ultrafast nonlinear TERS successes have utilized TECARS, a number of other advances have been made in the field. The Raschke group has combined ultrafast pulses with TERS tips not for ultrafast time resolution, but instead for excitation of surface plasmon polaritons (SPPs).[203] They have demonstrated the ability to couple plasmonic nanoscale tips with SPPs using ultrafast excitation for nanofocusing of femtosecond excitation beneath the tip with down to 10 nm spatial confinement.[204, 205] Significant progress has also been made in combining infrared spectroscopy with surface-enhancement towards many of the same goals as the ultrafast SERS field. These advances are well-reviewed elsewhere.[206-210] Combined with previous advances in ultrafast TERS, this work could pave the way for true nanoscale ultrafast spectroscopy.

The combination of ultrafast vibrational spectroscopies with the spatial resolution afforded by scanning probe microscopies (SPM) is on the forefront of this new ultrafast SERS field. It could eventually allow for the surface characterization and study of ultrafast dynamics of single molecules.

4. Overcoming the challenges of combining plasmonics and ultrafast spectroscopy

In many aspects, ultrafast SERS is currently transitioning from the initial proof of concept phase into routine spectroscopic experiments. As ultrafast SERS continues to develop, there are experimental challenges to keep in mind. This part of the review will discuss the major hurdles in the search for highly-enhancing plasmonic substrates that can withstand the intense peak powers present when using pico- and femtosecond pulsed lasers. First we address the challenges of substrate damage due to ultrafast pulses and molecular photodamage, along with the importance of sample characterization by showing damaged metallic nanostructures. Next we discuss potential solutions for the these challenges, including methods to minimize substrate damage, benefits of using high repetition rate / lower peak power laser systems, and favorable use of the electromagnetic field localization. Many of these damage mitigation techniques were critical to the successful ultrafast SERS experiments discussed in Section 3.

4.1 Morphological changes in nanostructures and molecular photodamage

4.1.1 Morphological changes in plasmonic nanostructures induced by ultrafast pulsed light

Ultrafast SERS typically utilizes inherently high peak powers to drive nonlinear processes that when coupled with plasmonic enhancement can lead to damage of the plasmonic substrate. Here we discuss this damage mechanism in more detail from a materials perspective.

Electron microscopy reports of plasmonically-enhanced damage in metal films by ultrafast pulses were first observed in macroscopic Pt gratings,[211], however the first changes of metal colloids caused by pico- and femtosecond pulsed lasers were observed in 1999.[26,

[212-215] The Kamat group witnessed a color change of thionicotinamide-functionalized gold nanosphere colloids after short (~1 min) durations of laser irradiation from the second harmonic of a Nd:YAG picosecond pulsed laser (532 nm, 18 ps bandwidth, 10 Hz, 1.5 mJ/pulse).[212] Using electron microscopy images, the authors showed that the nanoparticles underwent fusion, forming larger particles after irradiation. When the laser irradiation continued for ~30 min, fragmentation was observed.[212] The group of El-Sayed investigated the effect of femtosecond laser pulses on gold nanorods.[215] After irradiation at high laser fluences of ~ 1-10 J/cm^2 the particles fragmented and at lower fluences, 0.001 J/cm^2, the surface of the particles melted, as illustrated in Figures 14a and 14b. [26] The authors noted that the threshold for complete melting of the nanorods with fs laser pulses is about two orders of magnitude lower than that for ns excitation. These experiments paved the way to a better understanding of photodamage in plasmonic systems by demonstrating that electron microscopy can be used to illustrate the effects of high energy pulses on plasmonic materials.

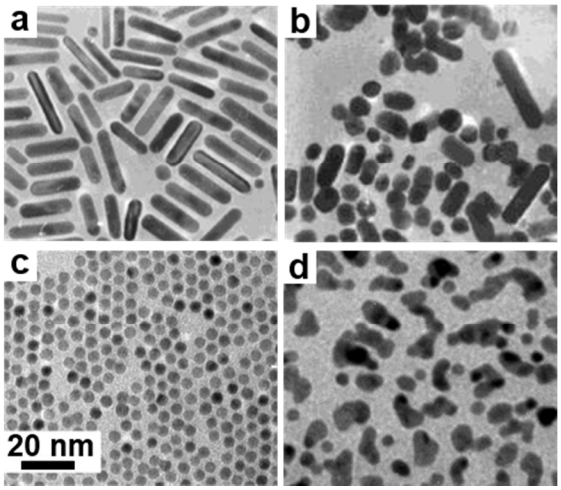

Figure 14. Transmission Electron Micrographs of gold colloids before (left) and after (right) laser irradiation. Top panel: (a) Gold nanorods before 800 nm femtosecond laser exposure (b) Resulting reshaped nanorods to more spheroidal particles with fluency of 0.001 J/cm^2. Adapted with permission from reference [26]. Copyright 2000 American Chemical Society. Lower panel: Spherical particles before (c) irradiation and after (d), illustrating sintering after exposing them to 300 nJ/pulse. Reprinted from reference [216]. Copyright 2004, with permission from Elsevier.

Laser fluence and pulse width are only two factors to consider when using ultrafast pulses with plasmonic particles. Colloid capping ligands and energetic overlap with the plasmon resonance of the particles can also have large effects. In a recent publication, Gordel et al. compared the photostability of CTAB-capped and sulfide-capped gold nanorods.[217] Using a Ti:sapphire system, the samples were irradiated with 800 nm, 130 fs pulses at 1 kHz with high (3.6 mJ/cm^2) and low (1.4 mJ/cm^2) fluences. In particular, the authors observed greater control of the reshaping and melting processes of sulfide-modified nanorods at low fluences compared to the highly nonuniform reshaping observed at high fluences. When sulfide-functionalized nanorods were illuminated with a laser wavelength on the rising spectral edge of the longitudinal LSPR mode, the size distribution of the

colloid could be narrowed; whereas with a laser wavelength at the longitudinal LSPR maximum, a new type of banana-shaped particles were formed.[217] Hence, the work of Gordel et al. suggests the possibility of controllable photoshaping of plasmonic substrates with selective capping ligands, laser fluence, and excitation resonance with the substrate LSPR.

Photodamage by pulsed laser light of metallodielectric core-shell colloids[218] and of metallic particles embedded in a solid matrix[219-222] have also been investigated. However, studies addressing the effect of ultrafast pulses on hot-spot dominated nanostructures such as coupled nanoparticles and particles with distinct and sharp nanofeatures (i.e. nanostars, concave cubes) are rare.[216, 223] In one such investigation, Eah et al. analyzed coupled metallic nanoparticles with femtosecond transient absorption spectroscopy.[216] At low pump power (150 nJ/pulse), the authors observed that the gold nanoparticle monolayer maintained its structural integrity, whereas at higher pump power (300 nJ/pulse), irreversible aggregation and sintering occurred (see Figures 15c and 15d).[216] Due to the high electric field confinement present in hot-spot dominated nanostructures, it will be valuable to extend the analysis of these systems in the presence of ultrafast radiation, particularly for thermodynamically unstable high surface curvature geometries. Understanding the reconstruction of these highly enhancing substrates that occur on the nanosecond timescale[224] is critical to developing better methods of preventing morphological changes so that ultrafast SERS techniques aren't limited to exceedingly short time windows or large colloidal sample volumes for data acquisition.

4.1.2 Molecular photodamage near nanostructures by ultrafast pulsed light

Just as plasmonic substrates can be damaged by plasmonically enhanced pico- and femtosecond pulses, molecules of interest in ultrafast SERS studies may be photodamaged. The damage may cause photobleaching or produce photoproducts that could complicate the spectral analysis. In their ultrafast SERS studies, Littleford et al. briefly mention that the energy densities (~0.6 mJ / cm^{-2}) they use should result in photodegradation, though they do not observe photoproducts.[225] As seen in Figure 15, Littleford et al. observed SERRS of 3,5-dimthoxy-4-(6'-azobenzotriazolyl)phenylamine (ABT-DMOPA) on Ag colloids taken with cw (Figure 15a) and pulsed (Figure 15b) excitations. To further explore different SERRS excitation conditions they performed an excitation power study. In CW excitation, the Raman intensity rises linearly with power, while the pulsed excitation (PL) shows a rapid saturation of Raman intensity with power. The authors suggest that with high-intensity laser pulses, the surface bonding between the metal surface and the analyte may be perturbed so that the dye diffuses away from the surface. They postulate that this not only perturbs the effects of chemical enhancement due to surface adsorption of the analyte on a plasmonic surface, but also decreases the electromagnetic enhancement due to the increased molecule-surface distance.

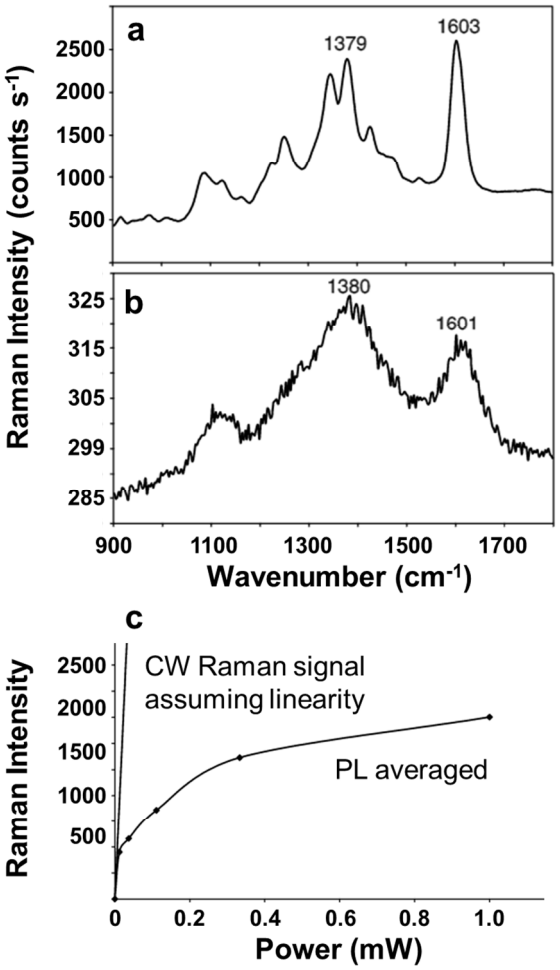

Figure 15. Comparison of SERRS of ABT-DMOPA on Ag colloids taken with cw (a) and pulsed (b) excitations: and the dependency of the Raman intensity to the excitation power for both conditions (c). CW excitation shows an expected linear trend with power, while the pulsed excitation (PL) shows a rapid saturation of Raman intensity with power, attributed to molecular photodamage. Adapted with permission from reference [225]. Copyright, 2005 John Wiley & Sons, Ltd.

In addition to perturbation of analyte adsorption and molecule diffusion, photobleaching due to pulsed excitation or plasmonically-enhanced fields can affect ultrafast SERS experiments.[226-228] It is important to note that photobleaching and photodamage of analytes does not always hamper plasmonic and ultrafast investigations. In fact, these phenomena have been used to study the intensity of plasmonically-enhanced fields,[163, 226] and may provide important information about field intensities when studying molecules in plasmonically-enhanced hot spots. While photodamage of analytes has been observed in recent ultrafast SERS applications, these effects have yet to be fully investigated, and importantly do not prevent new applications if the solutions discussed in the following section are considered.

In general, morphological changes in plasmonic nanostructures and molecular photodamage are sensitive to many experimental laser variables including laser wavelength, pulse duration,[212-215, 229] repetition rate,[212] fluence,[216, 225, 229] and irradiation

time.[212] In addition to the laser used, the morphological changes are also connected to the nanostructure including the composition, shape,[229] surface chemistry,[217] and energy of the LSPR relative to laser wavelength.[217] The conclusion of these studies suggest that close attention needs to be paid to nearly all laser and nanoparticle experimental variables when trying to control surface morphology changes and molecular photodamage by ultrafast laser pulses. Therefore, in the next section, we include some methods for mitigating such experimental limitations.

4.2 Solutions to provide robust molecule-plasmon systems for ultrafast pulsed experiments

4.2.1 Minimizing substrate damage in ultrafast pulsed experiments by protective coatings

Metallic nanoparticles are typically protected from ultrafast-laser-induced morphological degradation using monolayers of either strong capping agents including octanethiol,[230] octadecanethiol,[230] or oleylamine;[231] polymers,[79] or dielectric coatings.[232-238] Some of the more recent plasmonically enhanced coherent Raman scattering techniques, SEFSRS and TR-SECARS, have benefited from the use of silica-encapsulated gold aggregates.[9, 12, 175] These protective layers keep the plasmonic substrates more stable from thermal, mechanical and chemical degradation.[239, 240]

In particular, there is clear evidence on the enhanced photothermal robustness of silver nanoparticles with silica[240] and alumina coatings,[236] as well as silica coated gold nanorods [238] in ultrafast experimental applications.[237, 241] Sung et al. fabricated silver particle arrays by nanosphere lithography with different thicknesses of alumina coating: 0.0, 0.4, 1.0 nm; then exposed them to 90-fs, 1 kHz pulses of varied fluences. In this study, the laser wavelength was tuned in two ways: either (1) to match the LSPR extinction maximum, the *resonant* condition; or (2) ~100 nm red-shifted from the LSPR extinction maximum, the *off-resonant* condition. The photostability of the substrate was tracked by maximum wavelength and full width at half maximum (FWHM) of the LSPR at various exposure times (0-120 sec) and pulse fluences/energies (~0-2 mJ/cm^2). After just 30 sec of laser exposure, the authors observe a blue-shift in the LSPR band due to rounding of nanoparticle tips caused by laser heating effects. This effect was more pronounced as the laser pulse intensity increased and in resonant conditions since the absorption of the excitation pulses is more efficient on- than off-resonance. Advantageously, nanoparticle reshaping was mitigated by a factor of ten with a 1 nm thick alumina layer as depicted in Figure 16; presumably by increasing the surface-melting temperature. These results inform experimental design of ultrafast SERS experiments, suggesting protective coatings and off-resonant conditions to avoid sample degradation. These approaches have been successfully used in a few recent ultrafast SERS experiments as discussed in Section 3. For example, silica-coated nanoparticle aggregates were used in both SEFSRS[12, 175] and SECARS[9], and off-resonant pump pulses were used in SEFSRS[12, 175] and SECARS [9, 10] experiments to avoid unnecessary sample degradation.

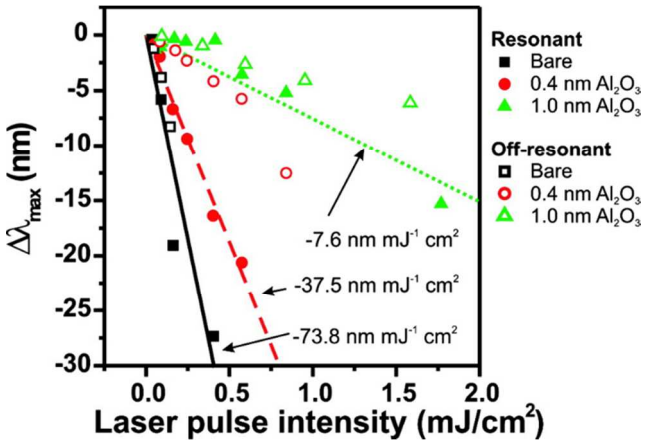

Figure 16. Effect of ultrafast excitation on bare and ALD coated Ag nanoparticles' optical properties. Blue shifts of LSPR maximum after 120 s of laser exposure versus laser pulse intensity. The resonant condition is plotted with solid marks, and the off-resonant condition is plotted with open marks. Linear fitting for the resonant condition is shown with solid black line, red dashed line, and green dotted line for bare particles, nanoparticles coated with 0.4 nm and 1.0 nm of Al_2O_3, respectively. Adapted with permission from reference [237]. Copyright 2008 American Chemical Society.

An alternative way to circumvent morphological damage of the substrate and/or molecular degradation by ultrafast lasers, is to utilize a flow cell.[225] By focusing the pulsed beam on a flowing jet of nanoparticles in solution during their ultrafast SERS experiments, Littleford et al. observed a significant decrease in sample degradation as compared to a static sample.[225] While circulating the sample usually requires a large volume of nanoparticles, which can restrict this approach for samples that are difficult or expensive to synthesize in bulk, continuous stirring of a small volume of sample in a cuvette can also prevent damage.[12]

In general when trying to mitigate photodamage of molecule-nanoparticle assemblies, the best physical methods used thus far include using various coatings over the entire assembly[9, 12, 175, 232-237] and continual replenishment.[225] More studies are need to determine how a protective mechanism may alter the desired experimental observable, depending on molecule-protective assembly-substrate interactions, However, these approaches can allow for more stable study of molecule-nanoparticle systems.

4.2.2 The role of higher repetition rate and lower peak power systems in ultrafast plasmonic studies

The results of the previous section imply that using lower peak power and higher repetition rate pulsed laser systems would allow for the expansion of ultrafast SERS techniques with limited signal saturation due to perturbation from pulsed excitation. This approach has allowed for the successful combination of SERS with ultrafast Raman techniques as the field has grown in the past decade. For example, the use of a higher repetition rate system with lower powers has been a major factor in the successful combination of SERS and FSRS[12, 175] when previous attempts had been unsuccessful likely due in part to sample photodegradation.[188] SECARS has also benefited from high repetition rate lasers: the Halas group used a 76 MHz system with low peak powers between 4-8 pJ /

pulse in their single molecule SECARS study,[10] while the Apkarian group used a 80 MHz system with peak powers between 4-12 pJ / pulse for their time-resolved single molecule SECARS study.[9] The lower peak powers provided by high repetition rate systems have been a boon to the ultrafast SERS community as previous work on just plasmonic substrates has shown peak powers in the tens to hundreds of nJ/pulse regime can lead to irreversible molecule-plasmon system damage.[216, 223]. By enabling a variety of successful ultrafast SERS experiments, it is anticipated that ultrafast SERS will continue to improve with the use of higher repetition rate systems.

4.2.3 Utilizing the effect of hot-spot distribution in ultrafast SERS applications

A significant progress in SERS came from revealing that the electromagnetic enhancement factor is typically an average value of a broad distribution of microscopic enhancement factors in different subsections of a substrate; and that a few molecules located at hot spots, where the electric field is highly enhanced, contribute disproportionally to the overall SERS signal.[45, 163, 242] In this regard, the Dlott group contributed significantly by providing measurements of the distribution of site specific enhancement factors on a silver film-over-nanospheres substrate.[163] Fang and coworkers used benzenethiol, a well characterized Raman scatterer, to show that the main contribution to the observed SERS enhancement was due to electromagnetic field enhancement rather than to chemical or resonance enhancements. Then, with a 532 nm picosecond pulsed laser the authors gradually photodamaged benzenethiol molecules at sites with highest electromagnetic enhancement by controlling the pulse energy; and to monitor the process by SERS they used a continuous wave 532 nm laser as a probe.[163] From their results, a distribution of microscopic enhancement factors was confirmed, hot spots with enhancement factors above 10^9 accounted for 63 ppm of the Raman scatterers but 24% of the overall SERS signal. The majority of the Raman scatterers were located at 'colder' sites with little contribution to the overall SERS signal.[163] This work suggests that the more locally-enhanced fields in hotspots could leave these areas of a substrate which contribute the most to the observed signal more prone to damage or molecular perturbation. This could explain observed signal decay in ultrafast SERS experiments such as SEFSRS, in which Frontiera et al. observed a loss of signal over time despite only small changes in the LSPR of the ensemble colloidal solution and negligible damage observed by HR-TEM.[175] However, it is also true that for ultrafast pulsed SERS applications, only a few of the most electromagnetically enhancing, or 'hottest', hot spots need to be able to withstand the pulsed excitation to observe signal. Examples of this include the TR-SECARS of Apkarian and SM-SECARS of Halas discussed earlier, where the majority of the signal, and the single molecule behavior, likely came from a particularly stable and highly enhancing hot spot.[9, 10]

The ultrafast SERS field has overcome many of the challenges caused by the combination of pulsed excitation and high-enhancing plasmonic substrates. In particular, approaches such as minimizing laser fluences,[216, 229] using protective surface coatings,[232-237] flowing colloidal SERS solutions,[12, 225] and moving towards higher repetition rate/lower peak power systems[9, 10, 12, 175] have advanced the field towards new directions beyond proof-of-principle demonstrations. Using a combination of substrate-molecule protective methods and the distribution of the Raman signal from very few molecules in highly enhancing electromagnetic hot spots has already produced ultrafast SERS studies

displaying single molecule behavior.[9, 10] It is expected that the field will continue to develop rapidly as more focus is placed on the molecule-substrate conditions in ultrafast SERS experiments.

5. Prospects for ultrafast SERS

The range of experiments described in Section 3 indicates that the ultrafast SERS field has significantly evolved in the last two decades. While not yet routine, ultrafast Raman measurements are now possible on a variety of plasmonic substrates and in a range of environments. This opens the door to a wide range of applications in sensing and the study of plasmon-mediated chemistry and physics.

The coherent nature of a number of these ultrafast SERS techniques could provide even higher sensitivity than typical SMSERS studies, opening to door to more analytes in a wider range of experimental conditions (off-resonance, non-ideal hotspots, less-enhancing substrates, etc.). The field of ultrafast SERS could grow with high-resolution microscopy expanding on TE-BB-CAR imaging[11] or with sensing applications utilizing the coherent nature of the ultrafast SERS techniques with multiple opportunities for plasmonically-enhanced interactions. Additionally, these techniques are uniquely suited to study the coupling of molecule and plasmons, as seen in SEFSRS.[12, 175] With the additional control afforded by UHV TERS environments,[202] these techniques could study the effects of molecular configuration and metal surface structure on the coupling of molecules and plasmons. It's clear that these techniques could be used to study dynamics of molecular subsets down to the single molecule level. However, it remains to be seen if studying single-molecule dynamics averaged over long many acquisitions will be more or less effective than carefully engineering highly homogenous subsets of molecules for dynamical studies. Either way, ultrafast SERS techniques hold the promise to combine extremely high sensitivity with ultrafast temporal resolution. But perhaps the most exciting use of ultrafast SERS is to study the dynamics of chemical reactions near plasmonic surfaces and the effects of the plasmons themselves on these reactions.

The ability to follow molecular structure as a function of time with ultrafast Raman spectroscopies on the picosecond or femtosecond time scale easily enables studies on the fundamental mechanisms of chemical reactions. Given the recent explosion of research in plasmonically-enhanced chemistry,[15-18, 56, 57, 90, 243-245] the combination of ultrafast Raman spectroscopies with plasmonic enhancements leaves the field of ultrafast SERS well-poised to answer questions regarding the mechanistic role of plasmons in such reactions. The now-mature fields of single molecule SERS,[3, 10] super-resolution SERS,[6, 246] and time-resolved SERS will be able to provide single hot spot (or possibly single-molecule) dynamic information. Surface plasmon resonances can assist reactions simply by electric field focusing and scattering, as well as by heat or modification of the molecular electronic distribution due to plexcitonic coupling.[247] Not long after the discovery of SERS, Nitzan et al. proposed that the highly concentrated electromagnetic fields present in SERS could be used to drive photochemical reactions.[248, 249] However, it is only recently that the field has developed a better understanding of the theory behind this phenomenon and experiments

with nanoscale-control of the necessary plasmonic properties.[15-18, 56, 57] Therefore the ultrafast studies mentioned in Sections 2 and 3 combined with the ready availability of plasmonic substrates through the ultraviolet, visible, and near infrared regimes will allow the field of ultrafast SERS to conclusively prove the potential and limitations of plasmons in driving chemistry.

Recent advances towards the use of plasmons to mediate photophysical processes have been nicely summarized in a recent reviews[13, 16, 17, 56, 57, 247] which describe different possible mechanisms for the functional role of plasmons in controlling (or not controlling) chemical reactions and photophysical processes. In semiconductor-noble metal hybrids such as TiO_2-M and ZnO-M (M=Au, Ag, Pd or Pt) the metal, size of the metal nanostructure and spectral range of light source used all affect the mechanism of plasmon-mediated charge-transfer.[13] For example, under UV light irradiation, small noble metal nanoparticles on the TiO_2 surface can trap electrons from the conduction band created by exciton transitions. This trapping consequently decreases the recombination rates during the interfacial charge transfer from the semiconductor to the metal.[13] It has also been observed that when semiconductor-noble metal hybrids are exposed to visible light, charge carriers in noble metals formed by the absorption of visible light, could be directly injected to the semiconductor. In this case, the excitation of the surface plasmon resonances initiates a charge transfer from the metal to the semiconductor if both materials are in close contact.[13] Alternative mechanisms of plasmon-mediated photocatalysis more directly linked to LSPR phenomena are those that rely on the concentration (near-field enhancement) and scattering of electromagnetic fields[13, 248, 249] or plasmonic heating effects.[56, 57, 247, 250, 251] These mechanisms have been exploited in photovoltaics and photocatalysis applications where TiO_2/ZnO–noble metal nanocomposites are used to enhance light absorption, light scattering, and photocurrent generation depending on the size of the plasmonic particle. But despite a number of studies to investigate the mechanisms of these plasmon-mediated photophysical or photochemical processes, a number of them are not well-understood.

The use of ultrafast SERS to examine nuclear and electronic motions on the femtosecond and picosecond time scale should shed light on the mechanism of plasmon-enhanced photochemistries such as the examples above for semiconductor-plasmonic nanocomposites. By obtaining structural snapshots on the ultrafast time scale, one can obtain the step-by-step process of bond-making, bond-breaking, and structural changes occurring in these molecule-plasmon systems. From a molecular point of view, the localized electromagnetic field may alter the reaction coordinate along the potential energy surface in different ways, altering the course of the reaction.[179, 181, 252] Short-lived bright plasmons,[253] or longer-lived dark plasmons[254, 255] may perturb this initial reaction coordinate, changing the outcome of a variety of photochemical processes. Hence, ultrafast SERS measurements on the single particle[162] and single molecule[9, 10, 136] levels can assist to elucidate which particle geometries are optimal for plasmon-enhanced chemistry, and how the structure of the particle and molecular configuration may affect the mechanism and yield of the photoreaction.

Time resolved SERS of single or few molecules is challenging due to sample degradation (as discussed in Section 4) and promising approaches typically involve a well-controlled environment or protective layers. A UHV environment minimizes oxygen-

induced degradation processes while enabling control over molecule-plasmon interactions with tip positioning. Additionally, ultrafast tip-enhanced Raman spectroscopy (TERS) spectroscopy combined with atomic level imaging by Scanning Tunneling Microscopy (STM), can lead to an unprecedented understanding of how molecules behave in site-specific environments with highly controlled electromagnetic fields. When combined with ultrafast SERS techniques discussed in Section 3, this could lead to major breakthroughs in understanding fundamental reaction mechanisms behind photovoltaic and photocatalytic composites, providing rational design principles for highly efficient plasmonically driven devices.

Alternative advancements in coupled molecule-plasmon studies may come from the combination of Raman spectroscopy and electron microscopy or pulse shaping techniques in order to directly image molecule-nanostructure on the femtosecond time scale. For example, coupling of ultrafast techniques to electron microscopy allowed for nm-scale spatial resolution and femtosecond time resolution of plasmonic energies utilizing electron energy loss spectroscopy (EELS).[256-258] Simultaneous control over spatial and temporal properties of electromagnetic fields scale has also been obtained based on the combination of polarization pulse shaping and time-resolved two-photon photoemission electron microscopy.[259-261] With this approach, the shaping of hot spots and visualization of surface plasmons on femtosecond time and nanometer length scales has already been demonstrated.[262-267] Although incorporating molecular imaging for molecules consisting primarily of light atoms presents significant technical difficulties, this could enable a real-time, real-space imaging of molecular plasmonic dynamics.

Now that the groundwork has been laid with recent developments in time-resolved and single molecule experiments, the field of ultrafast SERS is poised to study the mechanisms of plasmon-mediated chemistry, molecule-plasmon coupling, and the dynamics of single molecules.

6. Conclusions

Ultrafast SERS has developed at the intersection of ultrafast vibrational spectroscopy and plasmonics. The field has progressed significantly since early experiments, and it is clear that time-resolved experiments probing the dynamics of molecular-plasmonic systems nearing the single molecule limit are possible with possibly even higher sensitivity than spontaneous SERS experiments. These ultrafast SERS techniques are necessary to determine the functional role of plasmons in a variety of photovoltaic and photocatalytic devices, and will greatly assist in the optimization of robust, lightweight, and efficient light-driven chemical devices.

Ultrafast studies of plasmons and molecule-plasmon systems including transient absorption, SE-SHG, SE-SFG, SEHRS, SEFSRS, SECARS, TERS, and TECARS have shown promising results for understanding the nature of molecule-plasmon coupling. The strong molecule-plasmon energetic couplings observed in electronic spectroscopy along with the long-lived molecular coherent states near plasmonic surfaces demonstrate unique plasmonically-influenced time-resolved molecular dynamics. SEFSRS and SECARS have

both demonstrated high molecular sensitivity with time resolved dynamic signatures of molecule-plasmon interaction.[9, 10, 12, 173] Variations of SECARS are being pursued in coupled vibrational spectroscopy/scanning probe microscopy techniques as TECARS to push the spatial, temporal, spectral, and molecular concentration limits.[11, 162, 199] The SEFSRS and SECARS ultrafast SERS experiments are especially positioned to track plasmonically-enhanced chemistry *in-situ* by using optical fields to initiate photochemistry.

Overall, the field of ultrafast and nonlinear SERS have advanced greatly since early experiments several decades ago. Sample degradation was and will always remain a problem whenever plasmonic substrates with extremely high field enhancements are irradiated with pulsed excitation. However solutions such as silica coating, atomic layer deposition, and careful control of irradiation times, fluences, and repetition rates have resulted in the ability to routinely obtain SER spectra with pulsed excitation. New developments in combining existing ultrafast techniques with plasmonic materials now enable the real-time study of chemical reaction dynamics. This will provide an understanding of the effects of plasmonic fields, plasmon-generated hot electrons, and molecule-plasmon coupling effects, as well as leading to rational design principles in the development of devices, which utilize effects of plasmonic fields for chemistry. Finally, the advancements of ultrafast electron microscopy and ultrahigh vacuum TERS provide a pathway for spatial resolved ultrafast TERS, which will ultimately lead to following the spatiotemporally resolved dynamics of a single molecule under the influence of plasmonic fields.

ACKNOWLEDGMENTS

This work was supported by the National Science Foundation (CHE-1414466 and CHE-115247) and the Materials Research Center of Northwestern University (DMR-1121262). This work was supported by DARPA under SSC Pacific grants N660001–11–1-4179 and HR0011–13–2-002. Any opinions, findings, and conclusions or recommendations expressed in this publication are those of the author(s) and do not necessarily reflect the views of DARPA. NLG and MOM acknowledge support from the National Science Foundation Graduate Fellowship Research Program under Grant No. DGE-0824162.

1. D. L. Jeanmaire and R. P. Van Duyne, *Journal of Electroanalytical Chemistry and Interfacial Electrochemistry*, 1977, **84**, 1-20.
2. M. Albrecht and J. Creighton, *J. Am. Chem. Soc.*, 1977, **99**, 5215.
3. E. Le Ru, M. Meyer and P. Etchegoin, *The Journal of Physical Chemistry B*, 2006, **110**, 1944-1948.
4. J. A. Dieringer, R. B. Lettan, K. A. Scheidt and R. P. Van Duyne, *Journal of the American Chemical Society*, 2007, **129**, 16249-16256.
5. J. Steidtner and B. Pettinger, *Physical Review Letters*, 2008, **100**, 236101.
6. S. M. Stranahan and K. A. Willets, *Nano Letters*, 2010, **10**, 3777-3784.
7. K. A. Willets, *Chemical Society Reviews*, 2014, **43**, 3854-3864.

8. R. Zhang, Y. Zhang, Z. C. Dong, S. Jiang, C. Zhang, L. G. Chen, L. Zhang, Y. Liao, J. Aizpurua, Y. Luo, J. L. Yang and J. G. Hou, *Nature*, 2013, **498**, 82.
9. S. Yampolsky, D. A. Fishman, S. Dey, E. Hulkko, M. Banik, E. O. Potma and V. A. Apkarian, *Nature Photonics*, 2014, **8**, 650-656.
10. Y. Zhang, Y.-R. Zhen, O. Neumann, J. K. Day, P. Nordlander and N. J. Halas, *Nature communications*, 2014, **5**.
11. K. Furusawa, N. Hayazawa, F. C. Catalan, T. Okamoto and S. Kawata, *Journal of Raman Spectroscopy*, 2012, **43**, 656-661.
12. R. R. Frontiera, N. L. Gruenke and R. P. Van Duyne, *Nano Letters*, 2012, **12**, 5989-5994.
13. S. T. Kochuveedu, Y. H. Jang and D. H. Kim, *Chemical Society Reviews*, 2013, **42**, 8467-8493.
14. S. Mukherjee, L. Zhou, A. M. Goodman, N. Large, C. Ayala-Orozco, Y. Zhang, P. Nordlander and N. J. Halas, *Journal of the American Chemical Society*, 2014, **136**, 64-67.
15. P. Christopher, H. Xin, A. Marimuthu and S. Linic, *Nature materials*, 2012, **11**, 1044-1050.
16. W. Hou and S. B. Cronin, *Advanced Functional Materials*, 2013, **23**, 1612-1619.
17. K. Ueno and H. Misawa, *Journal of Photochemistry and Photobiology C: Photochemistry Reviews*, 2013, **15**, 31-52.
18. Z. Zhang, T. Deckert-Gaudig and V. Deckert, *Analyst*, 2015, **140**, 4325-4335.
19. A. H. Zewail, *Science*, 1988, **242**, 1645-1653.
20. G. Fleming, *Chemical applications of ultrafast spectroscopy*, 1986.
21. E. T. J. Nibbering, H. Fidder and E. Pines, *Annual Review of Physical Chemistry*, 2005, **56**, 337-367.
22. C. Fang, R. R. Frontiera, R. Tran and R. A. Mathies, *Nature*, 2009, **462**, 200-204.
23. C. Sönnichsen, T. Franzl, T. Wilk, G. von Plessen, J. Feldmann, O. Wilson and P. Mulvaney, *Physical Review Letters*, 2002, **88**, 077402.
24. H. Zhang and A. O. Govorov, *The Journal of Physical Chemistry C*, 2014, **118**, 7606-7614.
25. R. Sundararaman, P. Narang, A. S. Jermyn, W. A. Goddard Iii and H. A. Atwater, *Nat Commun*, 2014, **5**.
26. S. Link, C. Burda, B. Nikoobakht and M. A. El-Sayed, *The Journal of Physical Chemistry B*, 2000, **104**, 6152-6163.
27. S. A. Maier and H. A. Atwater, *Journal of Applied Physics*, 2005, **98**, 011101.
28. C. Clavero, *Nat Photon*, 2014, **8**, 95-103.
29. L. S and E.-S. MA, *J. Phys. Chem. B*, 1999, **103**, 8410.
30. T. S. Ahmadi, S. L. Logunov and M. A. El-Sayed, *The Journal of Physical Chemistry*, 1996, **100**, 8053-8056.
31. H. E. Elsayed-Ali, T. Juhasz, G. O. Smith and W. E. Bron, *Physical Review B*, 1991, **43**, 4488-4491.
32. G. V. Hartland, *Physical Chemistry Chemical Physics*, 2004, **6**, 5263-5274.
33. W. KA and V. D. RP, *Annu. Rev. Phys. Chem.*, 2007, **58**, 267.
34. P. L. Stiles, J. A. Dieringer, N. C. Shah, R. P. V. Duyne, J. DL and V. D. RP, *Annual Review of Analytical Chemistry*, 2008, **1**, 601-626.
35. B. Sharma, R. R. Frontiera, A.-I. Henry, E. Ringe and R. P. Van Duyne, *Materials Today*, 2012, **15**, 16-25.
36. R. F. Aroca, *Physical Chemistry Chemical Physics*, 2013, **15**, 5355-5363.
37. S. J. Lee, Z. Guan, H. Xu and M. Moskovits, *The Journal of Physical Chemistry C*, 2007, **111**, 17985-17988.
38. A. RF, A.-P. RA, P. N, S.-C. S and G.-R. JV, *Adv. Colloid Interface Sci.*, 2005, **116**, 45.
39. M. Moskovits, D. P. DiLella and K. J. Maynard, *Langmuir*, 1988, **4**, 67-76.
40. M. Moskovits and J. S. Suh, *The Journal of Physical Chemistry*, 1984, **88**, 5526-5530.

41. A. Otto, *Applications of Surface Science*, 1980, **6**, 309-355.
42. L. Jensen, C. M. Aikens and G. C. Schatz, *Chemical Society Reviews*, 2008, **37**, 1061-1073.
43. N. Valley, N. Greeneltch, R. P. Van Duyne and G. C. Schatz, *The Journal of Physical Chemistry Letters*, 2013, **4**, 2599-2604.
44. J. M. McMahon, S. Li, L. K. Ausman and G. C. Schatz, *The Journal of Physical Chemistry C*, 2012, **116**, 1627-1637.
45. E. Le Ru, E. Blackie, M. Meyer and P. G. Etchegoin, *The Journal of Physical Chemistry C*, 2007, **111**, 13794-13803.
46. J. P. Camden, J. A. Dieringer, Y. Wang, D. J. Masiello, L. D. Marks, G. C. Schatz and R. P. Van Duyne, *Journal of the American Chemical Society*, 2008, **130**, 12616-12617.
47. S. Shim, C. M. Stuart and R. A. Mathies, *ChemPhysChem*, 2008, **9**, 697-699.
48. E. C. L. Ru and P. G. Etchegoin, *Annual Review of Physical Chemistry*, 2012, **63**, 65-87.
49. R. A. Tripp, R. A. Dluhy and Y. Zhao, *Nano Today*, 2008, **3**, 31-37.
50. W. F. Paxton, S. L. Kleinman, A. N. Basuray, J. F. Stoddart and R. P. Van Duyne, *The Journal of Physical Chemistry Letters*, 2011, **2**, 1145-1149.
51. C. L. Brosseau, F. Casadio and R. P. Van Duyne, *Journal of Raman Spectroscopy*, 2011, **42**, 1305-1310.
52. B. Sharma, M. Fernanda Cardinal, S. L. Kleinman, N. G. Greeneltch, R. R. Frontiera, M. G. Blaber, G. C. Schatz and R. P. Van Duyne, *MRS Bulletin*, 2013, **38**, 615-624.
53. M. Moskovits, *Journal of Raman Spectroscopy*, 2005, **36**, 485-496.
54. M. Hu, H. Petrova, J. Chen, J. M. McLellan, A. R. Siekkinen, M. Marquez, X. Li, Y. Xia and G. V. Hartland, *The Journal of Physical Chemistry B*, 2006, **110**, 1520-1524.
55. G. Wu, A. Mikhailovsky, H. A. Khant, C. Fu, W. Chiu and J. A. Zasadzinski, *Journal of the American Chemical Society*, 2008, **130**, 8175-8177.
56. M. L. Brongersma, N. J. Halas and P. Nordlander, *Nat Nano*, 2015, **10**, 25-34.
57. M. Xiao, R. Jiang, F. Wang, C. Fang, J. Wang and J. C. Yu, *Journal of Materials Chemistry A*, 2013, **1**, 5790-5805.
58. L. Jing, W. Zhou, G. Tian and H. Fu, *Chemical Society Reviews*, 2013, **42**, 9509-9549.
59. A. Crut, P. Maioli, N. Del Fatti and F. Vallee, *Chemical Society Reviews*, 2014, **43**, 3921-3956.
60. L. Huang and J.-X. Cheng, *Annual Review of Materials Research*, 2013, **43**, 213-236.
61. S. S. Lo, M. S. Devadas, T. A. Major and G. V. Hartland, *Analyst*, 2013, **138**, 25-31.
62. G. V. Hartland, *Chemical Reviews*, 2011, **111**, 3858-3887.
63. G. V. Hartland, *Chemical Science*, 2010, **1**, 303-309.
64. G. V. Hartland, *Annu. Rev. Phys. Chem.*, 2006, **57**, 403.
65. S. Link and M. A. El-Sayed, *International Reviews in Physical Chemistry*, 2000, **19**, 409-453.
66. C. Voisin, N. Del Fatti, D. Christofilos and F. Vallée, *The Journal of Physical Chemistry B*, 2001, **105**, 2264-2280.
67. H. Harutyunyan, A. B. F. Martinson, D. Rosenmann, L. K. Khorashad, L. V. Besteiro, A. O. Govorov and G. P. Wiederrecht, *Nat Nano*, 2015, **10**, 770-774.
68. T. Stoll, P. Maioli, A. Crut, N. Del Fatti and F. Vallée, *Eur. Phys. J. B*, 2014, **87**, 1-19.
69. S. Link, C. Burda, Z. L. Wang and M. A. El-Sayed, *The Journal of Chemical Physics*, 1999, **111**, 1255-1264.
70. S. L. Westcott, R. D. Averitt, J. A. Wolfgang, P. Nordlander and N. J. Halas, *The Journal of Physical Chemistry B*, 2001, **105**, 9913-9917.
71. M. Pelton, J. E. Sader, J. Burgin, M. Liu, P. Guyot-Sionnest and D. Gosztola, *Nat Nano*, 2009, **4**, 492-495.

72. F. Banfi, V. Juve, D. Nardi, S. D. Conte, C. Giannetti, G. Ferrini, N. Del Fatti and F. Vallee, *Applied Physics Letters*, 2012, **100**, 011902-011903.
73. A. Warth, J. Lange, H. Graener and G. Seifert, *The Journal of Physical Chemistry C*, 2011, **115**, 23329-23337.
74. M. F. Cardinal, D. Mongin, A. l. Crut, P. Maioli, B. Rodríguez-González, J. Pérez-Juste, L. M. Liz-Marzán, N. Del Fatti and F. Vallée, *The Journal of Physical Chemistry Letters*, 2012, **3**, 613-619.
75. K. O. Aruda, M. Tagliazucchi, C. M. Sweeney, D. C. Hannah, G. C. Schatz and E. A. Weiss, *Proceedings of the National Academy of Sciences*, 2013, **110**, 4212-4217.
76. T. Stoll, P. Maioli, A. Crut, S. Rodal-Cedeira, I. Pastoriza-Santos, F. Vallée and N. Del Fatti, *The Journal of Physical Chemistry C*, 2015, **119**, 12757-12764.
77. S. Link and M. A. El-Sayed, *The Journal of Physical Chemistry B*, 1999, **103**, 8410-8426.
78. P. V. Kamat, M. Flumiani and G. V. Hartland, *The Journal of Physical Chemistry B*, 1998, **102**, 3123-3128.
79. H. Baida, D. Mongin, D. Christofilos, G. Bachelier, A. Crut, P. Maioli, N. Del Fatti and F. Vallée, *Physical review letters*, 2011, **107**, 057402.
80. R. Marty, A. Arbouet, C. Girard, A. Mlayah, V. Paillard, V. K. Lin, S. L. Teo and S. Tripathy, *Nano Letters*, 2011, **11**, 3301-3306.
81. M. Pelton, M. Liu, S. Park, N. F. Scherer and P. Guyot-Sionnest, *Physical Review B*, 2006, **73**, 155419.
82. P. Zijlstra, A. L. Tchebotareva, J. W. M. Chon, M. Gu and M. Orrit, *Nano Letters*, 2008, **8**, 3493-3497.
83. P. V. Ruijgrok, P. Zijlstra, A. L. Tchebotareva and M. Orrit, *Nano Letters*, 2012, **12**, 1063-1069.
84. F. Masia, W. Langbein and P. Borri, *Physical Chemistry Chemical Physics*, 2013, **15**, 4226-4232.
85. T. A. Major, A. Crut, B. Gao, S. S. Lo, N. D. Fatti, F. Vallee and G. V. Hartland, *Physical Chemistry Chemical Physics*, 2013, **15**, 4169-4176.
86. T. Schumacher, K. Kratzer, D. Molnar, M. Hentschel, H. Giessen and M. Lippitz, *Nat Commun*, 2011, **2**, 333.
87. J. Burgin, P. Langot, N. Del Fatti, F. Vallée, W. Huang and M. A. El-Sayed, *The Journal of Physical Chemistry C*, 2008, **112**, 11231-11235.
88. L. Wang, Y. Nishijima, K. Ueno, H. Misawa and N. Tamai, *The Journal of Physical Chemistry C*, 2012, **116**, 17838-17846.
89. N. Large, L. Saviot, J. r. m. Margueritat, J. Gonzalo, C. N. Afonso, A. Arbouet, P. Langot, A. Mlayah and J. Aizpurua, *Nano Letters*, 2009, **9**, 3732-3738.
90. E. L. Keller, N. C. Brandt, A. A. Cassabaum and R. R. Frontiera, *Analyst*, 2015, **140**, 4922-4931.
91. N. Zohar, L. Chuntonov and G. Haran, *Journal of Photochemistry and Photobiology C: Photochemistry Reviews*, 2014, **21**, 26-39.
92. P. Törmä and W. L. Barnes, *Reports on Progress in Physics*, 2015, **78**, 013901.
93. A. Salomon, C. Genet and T. W. Ebbesen, *Angewandte Chemie International Edition*, 2009, **48**, 8748-8751.
94. N. T. Fofang, N. K. Grady, Z. Fan, A. O. Govorov and N. J. Halas, *Nano Letters*, 2011, **11**, 1556-1560.
95. A. O. Govorov, H. Zhang and Y. K. Gun'ko, *The Journal of Physical Chemistry C*, 2013, **117**, 16616-16631.

96. A. O. Govorov, G. W. Bryant, W. Zhang, T. Skeini, J. Lee, N. A. Kotov, J. M. Slocik and R. R. Naik, *Nano Letters*, 2006, **6**, 984-994.
97. T. Uwada, R. Toyota, H. Masuhara and T. Asahi, *The Journal of Physical Chemistry C*, 2007, **111**, 1549-1552.
98. G. P. Wiederrecht, G. A. Wurtz and A. Bouhelier, *Chemical Physics Letters*, 2008, **461**, 171-179.
99. J. Hranisavljevic, N. M. Dimitrijevic, G. A. Wurtz and G. P. Wiederrecht, *Journal of the American Chemical Society*, 2002, **124**, 4536-4537.
100. G. P. Wiederrecht, G. A. Wurtz and J. Hranisavljevic, *Nano Letters*, 2004, **4**, 2121-2125.
101. T. J. Antosiewicz, S. P. Apell and T. Shegai, *ACS Photonics*, 2014, **1**, 454-463.
102. G. Zengin, M. Wersäll, S. Nilsson, T. J. Antosiewicz, M. Käll and T. Shegai, *Physical review letters*, 2015, **114**, 157401.
103. S. Balci, C. Kocabas, B. Küçüköz, A. Karatay, E. Akhüseyin, H. G. Yaglioglu and A. Elmali, *Applied Physics Letters*, 2014, **105**, 051105.
104. S. Balci, E. Karademir, C. Kocabas and A. Aydinli, *Optics Letters*, 2014, **39**, 4994-4997.
105. W. Wang, P. Vasa, R. Pomraenke, R. Vogelgesang, A. De Sio, E. Sommer, M. Maiuri, C. Manzoni, G. Cerullo and C. Lienau, *ACS Nano*, 2014, **8**, 1056-1064.
106. A. I. Väkeväinen, R. J. Moerland, H. T. Rekola, A. P. Eskelinen, J. P. Martikainen, D. H. Kim and P. Törmä, *Nano Letters*, 2014, **14**, 1721-1727.
107. B. G. DeLacy, O. D. Miller, C. W. Hsu, Z. Zander, S. Lacey, R. Yagloski, A. W. Fountain, E. Valdes, E. Anquillare, M. Soljačić, S. G. Johnson and J. D. Joannopoulos, *Nano Letters*, 2015, **15**, 2588-2593.
108. F. Nan, Y.-F. Zhang, X. Li, X.-T. Zhang, H. Li, X. Zhang, R. Jiang, J. Wang, W. Zhang, L. Zhou, J.-H. Wang, Q.-Q. Wang and Z. Zhang, *Nano Letters*, 2015, **15**, 2705-2710.
109. T. Itoh, Y. S. Yamamoto, H. Tamaru, V. Biju, S.-i. Wakida and Y. Ozaki, *Physical Review B*, 2014, **89**, 195436.
110. A. E. Schlather, N. Large, A. S. Urban, P. Nordlander and N. J. Halas, *Nano Letters*, 2013, **13**, 3281-3286.
111. K. Katayama, K. Shibamoto and T. Sawada, *Chemical Physics Letters*, 2001, **345**, 265-271.
112. K. Shibamoto, K. Katayama and T. Sawada, *Chemical Physics Letters*, 2007, **433**, 385-389.
113. H. Gersen, M. F. García-Parajó, L. Novotny, J. A. Veerman, L. Kuipers and N. F. van Hulst, *Physical Review Letters*, 2000, **85**, 5312-5315.
114. R. C. Maher, C. M. Galloway, E. C. Le Ru, L. F. Cohen and P. G. Etchegoin, *Chemical Society Reviews*, 2008, **37**, 965-979.
115. K. Kneipp, Y. Wang, H. Kneipp, I. Itzkan, R. R. Dasari and M. S. Feld, *Physical Review Letters*, 1996, **76**, 2444-2447.
116. V. Kozich and W. Werncke, *The Journal of Physical Chemistry C*, 2010, **114**, 10484-10488.
117. B. Levine, C. V. Shank and J. P. Heritage, *Quantum Electronics, IEEE Journal of*, 1979, **15**, 1418-1432.
118. P. Matousek, M. Towrie, A. Stanley and A. Parker, *Applied Spectroscopy*, 1999, **53**, 1485-1489.
119. P. Matousek, M. Towrie, C. Ma, W. M. Kwok, D. Phillips, W. T. Toner and A. W. Parker, *Journal of Raman Spectroscopy*, 2001, **32**, 983-988.
120. J. P. Heritage and D. L. Allara, *Chemical Physics Letters*, 1980, **74**, 507-510.
121. H. Arnolds, *Progress in Surface Science*, 2011, **86**, 1-40.
122. H. Arnolds and M. Bonn, *Surface Science Reports*, 2010, **65**, 45-66.
123. C. D. Bain, *Journal of the Chemical Society, Faraday Transactions*, 1995, **91**, 1281-1296.

124. I. V. Stiopkin, H. D. Jayathilake, A. N. Bordenyuk and A. V. Benderskii, *Journal of the American Chemical Society*, 2008, **130**, 2271-2275.
125. J. A. Carter, Z. Wang and D. D. Dlott, *Accounts of Chemical Research*, 2009, **42**, 1343-1351.
126. C. K. Chen, T. F. Heinz, D. Ricard and Y. R. Shen, *Physical Review B*, 1983, **27**, 1965-1979.
127. A. N. Bordenyuk, C. Weeraman, A. Yatawara, H. D. Jayathilake, I. Stiopkin, Y. Liu and A. V. Benderskii, *The Journal of Physical Chemistry C*, 2007, **111**, 8925-8933.
128. C. Weeraman, A. K. Yatawara, A. N. Bordenyuk and A. V. Benderskii, *Journal of the American Chemical Society*, 2006, **128**, 14244-14245.
129. O. Pluchery, C. Humbert, M. Valamanesh, E. Lacaze and B. Busson, *Physical Chemistry Chemical Physics*, 2009, **11**, 7729-7737.
130. S. Baldelli, A. S. Eppler, E. Anderson, Y.-R. Shen and G. A. Somorjai, *The Journal of Chemical Physics*, 2000, **113**, 5432-5438.
131. K. Tsuboi, S. Abe, S. Fukuba, M. Shimojo, M. Tanaka, K. Furuya, K. Fujita and K. Kajikawa, *The Journal of Chemical Physics*, 2006, **125**, -.
132. T. Kawai, D. J. Neivandt and P. B. Davies, *J. Am. Chem. Soc.*, 2000, **122**, 12031.
133. T. Gérard, D. Laurent, V. Cedric, S. Yannick, A. T. Paul and P. André, *Nanotechnology*, 2007, **18**, 415301.
134. Q. Li, C. W. Kuo, Z. Yang, P. Chen and K. C. Chou, *Physical Chemistry Chemical Physics*, 2009, **11**, 3436-3442.
135. J. Kneipp, H. Kneipp and K. Kneipp, *Proceedings of the National Academy of Sciences*, 2006, **103**, 17149-17153.
136. C. B. Milojevich, B. K. Mandrell, H. K. Turley, V. Iberi, M. D. Best and J. P. Camden, *The Journal of Physical Chemistry Letters*, 2013, **4**, 3420-3423.
137. K. Kneipp, H. Kneipp and F. Seifert, *Chemical physics letters*, 1995, **233**, 519-524.
138. A. M. Kelley, *Annual review of physical chemistry*, 2010, **61**, 41-61.
139. J. T. Golab, J. R. Sprague, K. T. Carron, G. C. Schatz and R. P. Van Duyne, *The Journal of Chemical Physics*, 1988, **88**, 7942-7951.
140. S. Nie, L. A. Lipscomb, S. Feng and N.-T. Yu, *Chemical Physics Letters*, 1990, **167**, 35-40.
141. L. A. Lipscomb, S. Nie, S. Feng and N.-T. Yu, *Chemical Physics Letters*, 1990, **170**, 457-461.
142. H. Kneipp, K. Kneipp and F. Seifert, *Chemical physics letters*, 1993, **212**, 374-378.
143. C. B. Milojevich, D. W. Silverstein, L. Jensen and J. P. Camden, *ChemPhysChem*, 2011, **12**, 101-103.
144. H. Turley and J. Camden, *Chemical Communications*, 2014, **50**, 1472-1474.
145. K. König, *Journal of microscopy*, 2000, **200**, 83-104.
146. R. W. Boyd, *Nonlinear optics*, Academic press, 2003.
147. P. Maker and R. Terhune, *Physical Review*, 1965, **137**, A801.
148. M. D. Duncan, J. Reintjes and T. Manuccia, *Optics letters*, 1982, **7**, 350-352.
149. A. Zumbusch, G. R. Holtom and X. S. Xie, *Physical Review Letters*, 1999, **82**, 4142.
150. G. W. Wurpel, J. M. Schins and M. Müller, *Optics letters*, 2002, **27**, 1093-1095.
151. C. L. Evans, E. O. Potma, M. Puoris' haag, D. Côté, C. P. Lin and X. S. Xie, *Proceedings of the National Academy of Sciences of the United States of America*, 2005, **102**, 16807-16812.
152. C. L. Evans and X. S. Xie, *Annu. Rev. Anal. Chem.*, 2008, **1**, 883-909.
153. J. P. Pezacki, J. A. Blake, D. C. Danielson, D. C. Kennedy, R. K. Lyn and R. Singaravelu, *Nature chemical biology*, 2011, **7**, 137-145.
154. J. P. Day, K. F. Domke, G. Rago, H. Kano, H.-o. Hamaguchi, E. M. Vartiainen and M. Bonn, *The Journal of Physical Chemistry B*, 2011, **115**, 7713-7725.
155. J.-X. Cheng and X. S. Xie, *The Journal of Physical Chemistry B*, 2004, **108**, 827-840.
156. L. Piatkowski, J. T. Hugall and N. F. van Hulst, *Nature Photonics*, 2014, **8**, 589-591.

157. C. Chen, A. De Castro, Y. Shen and F. DeMartini, *Physical Review Letters*, 1979, **43**, 946.
158. T.-W. Koo, S. Chan and A. A. Berlin, *Optics letters*, 2005, **30**, 1024-1026.
159. E. Liang, A. Weippert, J.-M. Funk, A. Materny and W. Kiefer, *Chemical physics letters*, 1994, **227**, 115-120.
160. P. Lee and D. Meisel, *The Journal of Physical Chemistry*, 1982, **86**, 3391-3395.
161. J.-x. Cheng, A. Volkmer, L. D. Book and X. S. Xie, *The Journal of Physical Chemistry B*, 2001, **105**, 1277-1280.
162. T. Ichimura, N. Hayazawa, M. Hashimoto, Y. Inouye and S. Kawata, *Journal of Raman Spectroscopy*, 2003, **34**, 651-654.
163. Y. Fang, N.-H. Seong and D. D. Dlott, *Science*, 2008, **321**, 388-392.
164. S. Schlücker, M. Salehi, G. Bergner, M. Schütz, P. Ströbel, A. Marx, I. Petersen, B. Dietzek and J. r. Popp, *Analytical chemistry*, 2011, **83**, 7081-7085.
165. C. J. Addison, S. O. Konorov, A. G. Brolo, M. W. Blades and R. F. Turner, *The Journal of Physical Chemistry C*, 2009, **113**, 3586-3592.
166. C. Steuwe, C. F. Kaminski, J. J. Baumberg and S. Mahajan, *Nano letters*, 2011, **11**, 5339-5343.
167. H. Chew, D. Wang and M. Kerker, *JOSA B*, 1984, **1**, 56-66.
168. J. A. Parkhill, D. Rappoport and A. Aspuru-Guzik, *The Journal of Physical Chemistry Letters*, 2011, **2**, 1849-1854.
169. X. Hua, D. V. Voronine, C. W. Ballmann, A. M. Sinyukov, A. V. Sokolov and M. O. Scully, *Physical Review A*, 2014, **89**, 043841.
170. D. V. Voronine, A. M. Sinyukov, X. Hua, E. Munusamy, G. Ariunbold, A. V. Sokolov and M. O. Scully, *Journal of Modern Optics*, 2015, **62**, 90-96.
171. A. J. Moad and G. J. Simpson, *The Journal of Physical Chemistry A*, 2005, **109**, 1316-1323.
172. S. Mukamel, *Principles of nonlinear optical spectroscopy*, Oxford University Press, 1999.
173. D. V. Voronine, A. M. Sinyukov, X. Hua, K. Wang, P. K. Jha, E. Munusamy, S. E. Wheeler, G. Welch, A. V. Sokolov and M. O. Scully, *Scientific reports*, 2012, **2**.
174. M. Scully, G. Kattawar, R. Lucht, T. Opatrný, H. Pilloff, A. Rebane, A. Sokolov and M. Zubairy, *Proceedings of the National Academy of Sciences*, 2002, **99**, 10994-11001.
175. R. R. Frontiera, A.-I. Henry, N. L. Gruenke and R. P. Van Duyne, *The Journal of Physical Chemistry Letters*, 2011, **2**, 1199-1203.
176. P. Kukura, S. Yoon and R. A. Mathies, *Analytical Chemistry*, 2006, **78**, 5952-5959.
177. P. Kukura, D. W. McCamant and R. A. Mathies, *Annual Review of Physical Chemistry*, 2007, **58**, 461-488.
178. R. R. Frontiera and R. A. Mathies, *Laser & Photonics Reviews*, 2011, **5**, 102-113.
179. P. Kukura, D. W. McCamant, S. Yoon, D. B. Wandschneider and R. A. Mathies, *Science*, 2005, **310**, 1006-1009.
180. D. W. McCamant, P. Kukura and R. A. Mathies, *The Journal of Physical Chemistry B*, 2005, **109**, 10449-10457.
181. J. Dasgupta, R. R. Frontiera, K. C. Taylor, J. C. Lagarias and R. A. Mathies, *Proceedings of the National Academy of Sciences*, 2009, **106**, 1784-1789.
182. D. W. McCamant, P. Kukura and R. A. Mathies, *The journal of physical chemistry. A*, 2003, **107**, 8208-8214.
183. R. R. Frontiera, J. Dasgupta and R. A. Mathies, *Journal of the American Chemical Society*, 2009, **131**, 15630-15632.
184. K. E. Brown, B. S. Veldkamp, D. T. Co and M. R. Wasielewski, *The Journal of Physical Chemistry Letters*, 2012, **3**, 2362-2366.

185. F. Provencher, N. Bérubé, A. W. Parker, G. M. Greetham, M. Towrie, C. Hellmann, M. Côté, N. Stingelin, C. Silva and S. C. Hayes, *Nat Commun*, 2014, **5**.
186. W. Yu, P. J. Donohoo-Vallett, J. Zhou and A. E. Bragg, *The Journal of Chemical Physics*, 2014, **141**, 044201.
187. S. Yoon, P. Kukura, C. M. Stuart and R. A. Mathies, *Molecular Physics*, 2006, **104**, 1275-1282.
188. E. C. Ploetz, M. Gellner, M. Schütz, B. Marx, S. Schlücker and P. Gilch, *AIP Conference Proceedings*, 2010, **1267**, 88-89.
189. B. Knoll and F. Keilmann, *Nature*, 1999, **399**, 134-137.
190. B. C. Stipe, M. A. Rezaei and W. Ho, *Science*, 1998, **280**, 1732.
191. R. Hillenbrand, T. Taubner and F. Keilmann, *Nature*, 2002, **418**, 159-162.
192. C. C. Neacsu, J. Dreyer, N. Behr and M. B. Raschke, *Physical Review B*, 2006, **73**, 193406.
193. J. M. Klingsporn, M. D. Sonntag, T. Seideman and R. P. Van Duyne, *The Journal of Physical Chemistry Letters*, 2014, **5**, 106-110.
194. E. A. Pozzi, M. D. Sonntag, N. Jiang, J. M. Klingsporn, M. C. Hersam and R. P. Van Duyne, *ACS Nano*, 2013, **7**, 885-888.
195. Z. D. Schultz, J. M. Marr and H. Wang, *Nanophotonics*, 2014, **3**, 91-104.
196. M. D. Sonntag, E. A. Pozzi, N. Jiang, M. C. Hersam and R. P. Van Duyne, *The Journal of Physical Chemistry Letters*, 2014, **5**, 3125-3130.
197. M. D. Sonntag, J. M. Klingsporn, L. K. Garibay, J. M. Roberts, J. A. Dieringer, T. Seideman, K. A. Scheidt, L. Jensen, G. C. Schatz and R. P. Van Duyne, *J. Phys. Chem. C*, 2012, **116**, 478.
198. A. Hartschuh, E. J. Sánchez, X. S. Xie and L. Novotny, *Physical Review Letters*, 2003, **90**, 095503.
199. T. Ichimura, N. Hayazawa, M. Hashimoto, Y. Inouye and S. Kawata, *Physical Review Letters*, 2004, **92**, 220801.
200. T. Ichimura, N. Hayazawa, M. Hashimoto, Y. Inouye and S. Kawata, *Applied Physics Letters*, 2004, **84**, 1768-1770.
201. N. Hayazawa, T. Ichimura, M. Hashimoto, Y. Inouye and S. Kawata, *Journal of Applied Physics*, 2004, **95**, 2676-2681.
202. E. A. Pozzi, M. D. Sonntag, N. Jiang, N. Chiang, T. Seideman, M. C. Hersam and R. P. Van Duyne, *The Journal of Physical Chemistry Letters*, 2014, **5**, 2657-2661.
203. S. Berweger, J. M. Atkin, R. L. Olmon and M. B. Raschke, *The Journal of Physical Chemistry Letters*, 2012, **3**, 945-952.
204. X. G. Xu, M. Rang, I. M. Craig and M. B. Raschke, *The Journal of Physical Chemistry Letters*, 2012, **3**, 1836-1841.
205. X. G. Xu and M. B. Raschke, *Nano Letters*, 2013, **13**, 1588-1595.
206. J. M. Atkin, S. Berweger, A. C. Jones and M. B. Raschke, *Advances in Physics*, 2012, **61**, 745-842.
207. E. A. Muller, B. Pollard and M. B. Raschke, *The Journal of Physical Chemistry Letters*, 2015, **6**, 1275-1284.
208. L.-X. Wang and X.-E. Jiang, *Chinese Journal of Analytical Chemistry*, 2012, **40**, 975-982.
209. D. A. Schmidt, I. Kopf and E. Bründermann, *Laser & Photonics Reviews*, 2012, **6**, 296-332.
210. E. Brundermann and M. Havenith, *Annual Reports Section "C" (Physical Chemistry)*, 2008, **104**, 235-255.
211. K. L. Haller, L. A. Bumm, R. I. Altkorn, E. J. Zeman, G. C. Schatz and R. P. Van Duyne, *The Journal of Chemical Physics*, 1989, **90**, 1237-1252.
212. H. Fujiwara, S. Yanagida and P. V. Kamat, *The Journal of Physical Chemistry B*, 1999, **103**, 2589-2591.

213. N. Chandrasekharan, P. V. Kamat, J. Hu and G. Jones, *The Journal of Physical Chemistry B*, 2000, **104**, 11103-11109.
214. S. Link, C. Burda, B. Nikoobakht and M. El-Sayed, *Chemical Physics Letters*, 1999, **315**, 12-18.
215. S. Link, C. Burda, M. Mohamed, B. Nikoobakht and M. El-Sayed, *The Journal of Physical Chemistry A*, 1999, **103**, 1165-1170.
216. S.-K. Eah, H. M. Jaeger, N. F. Scherer, X.-M. Lin and G. P. Wiederrecht, *Chemical physics letters*, 2004, **386**, 390-395.
217. M. Gordel, J. Olesiak-Banska, K. Matczyszyn, C. Nogues, M. Buckle and M. Samoc, *Phys. Chem. Chem. Phys.*, 2013, **16**, 71-78.
218. F. Tam, C. Moran and N. Halas, *The Journal of Physical Chemistry B*, 2004, **108**, 17290-17294.
219. G. Seifert, M. Kaempfe, K.-J. Berg and H. Graener, *Applied Physics B*, 2000, **71**, 795-800.
220. H. Graener, G. Seifert, A. Podlipensky, B. Sepiol and M. Leitner, 2007.
221. A. Stalmashonak, H. Graener and G. Seifert, *Applied Physics Letters*, 2009, **94**, 193111.
222. J. Doster, G. Baraldi, J. Gonzalo, J. Solis, J. Hernandez-Rueda and J. Siegel, *Applied Physics Letters*, 2014, **104**, 153106.
223. N. K. Grady, M. W. Knight, R. Bardhan and N. J. Halas, *Nano letters*, 2010, **10**, 1522-1528.
224. K. Kleiner, A. Comas-Vives, M. Naderian, J. E. Mueller, D. Fantauzzi, M. Mesgar, J. A. Keith, J. Anton and T. Jacob, *Advances in Physical Chemistry*, 2011, **2011**, 11.
225. R. E. Littleford, D. Cunningham, P. Matousek, M. Towrie, A. W. Parker, I. Khan, D. McComb and W. Ewen Smith, *Journal of Raman Spectroscopy*, 2005, **36**, 600-605.
226. B. Pettinger, B. Ren, G. Picardi, R. Schuster and G. Ertl, *Journal of Raman Spectroscopy*, 2005, **36**, 541-550.
227. K. Toyota, S. Nakashima and T. Okada, *Chemical Physics Letters*, 2000, **323**, 323-328.
228. E. Le Ru, P. Etchegoin and M. Meyer, *The Journal of chemical physics*, 2006, **125**, 204701.
229. S. Link, Z. L. Wang and M. A. El-Sayed, *The Journal of Physical Chemistry B*, 2000, **104**, 7867-7870.
230. R. Philip, G. R. Kumar, N. Sandhyarani and T. Pradeep, *Physical Review B*, 2000, **62**, 13160.
231. L. Polavarapu, N. Venkatram, W. Ji and Q.-H. Xu, *ACS applied materials & interfaces*, 2009, **1**, 2298-2303.
232. M. Nisoli, S. De Silvestri, A. Cavalleri, A. Malvezzi, A. Stella, G. Lanzani, P. Cheyssac and R. Kofman, *Physical Review B*, 1997, **55**, R13424.
233. H. Baida, D. Christofilos, P. Maioli, A. Crut, N. Del Fatti and F. Vallée, *Journal of Raman Spectroscopy*, 2011, **42**, 1891-1896.
234. X. Cui, D. Erni, W. Zhang and R. Zenobi, *Chemical Physics Letters*, 2008, **453**, 262-265.
235. G. Polizos, E. Tuncer, A. L. Agapov, D. Stevens, A. P. Sokolov, M. Kidder, J. Jacobs, H. Koerner, R. Vaia and K. More, *Polymer*, 2012, **53**, 595-603.
236. A. V. Whitney, J. W. Elam, P. C. Stair and R. P. Van Duyne, *The Journal of Physical Chemistry C*, 2007, **111**, 16827-16832.
237. J. Sung, K. M. Kosuda, J. Zhao, J. W. Elam, K. G. Spears and R. P. Van Duyne, *The Journal of Physical Chemistry C*, 2008, **112**, 5707-5714.
238. X.-D. Wang, A.-P. Luo, H. Liu, N. Zhao, M. Liu, Y.-F. Zhu, J.-P. Xue, Z.-C. Luo and W.-C. Xu, *Opt. Express*, 2015, **23**, 22602-22610.
239. C. A. Barrios, A. V. Malkovskiy, R. D. Hartschuh, A. M. Kisliuk, A. P. Sokolov and M. D. Foster, 2008.
240. X. Li, J.-P. Lee, K. S. Blinn, D. Chen, S. Yoo, B. Kang, L. A. Bottomley, M. A. El-Sayed, S. Park and M. Liu, *Energy & Environmental Science*, 2014, **7**, 306-310.

241. S. L. Kleinman, B. Sharma, M. G. Blaber, A.-I. Henry, N. Valley, R. G. Freeman, M. J. Natan, G. C. Schatz and R. P. Van Duyne, *Journal of the American Chemical Society*, 2012, **135**, 301-308.
242. D. P. dos Santos, M. L. Temperini and A. G. Brolo, *Journal of the American Chemical Society*, 2012, **134**, 13492-13500.
243. P. Christopher, H. Xin and S. Linic, *Nat Chem*, 2011, **3**, 467-472.
244. S. Linic, P. Christopher and D. B. Ingram, *Nat Mater*, 2011, **10**, 911-921.
245. Z. Liu, W. Hou, P. Pavaskar, M. Aykol and S. B. Cronin, *Nano Letters*, 2011, **11**, 1111-1116.
246. E. J. Titus, M. L. Weber, S. M. Stranahan and K. A. Willets, *Nano Letters*, 2012, **12**, 5103-5110.
247. G. Baffou and R. Quidant, *Chemical Society Reviews*, 2014, **43**, 3898-3907.
248. A. Nitzan and L. E. Brus, *The Journal of Chemical Physics*, 1981, **74**, 5321-5322.
249. A. Nitzan and L. E. Brus, *The Journal of Chemical Physics*, 1981, **75**, 2205-2214.
250. X.-J. Chen, G. Cabello, D.-Y. Wu and Z.-Q. Tian, *Journal of Photochemistry and Photobiology C: Photochemistry Reviews*, 2014, **21**, 54-80.
251. S. Bai, J. Jiang, Q. Zhang and Y. Xiong, *Chemical Society Reviews*, 2015, **44**, 2893-2939.
252. S. Shim, J. Dasgupta and R. A. Mathies, *Journal of the American Chemical Society*, 2009, **131**, 7592-7597.
253. K. O. Aruda, M. Tagliazucchi, C. M. Sweeney, D. C. Hannah and E. A. Weiss, *Physical Chemistry Chemical Physics*, 2013, **15**, 7441-7449.
254. D. E. Gómez, Z. Q. Teo, M. Altissimo, T. J. Davis, S. Earl and A. Roberts, *Nano Letters*, 2013, **13**, 3722-3728.
255. S. L. Kleinman, B. Sharma, M. G. Blaber, A.-I. Henry, N. Valley, R. G. Freeman, M. J. Natan, G. C. Schatz and R. P. Van Duyne, *Journal of the American Chemical Society*, 2013, **135**, 301-308.
256. A. Yurtsever, R. M. van der Veen and A. H. Zewail, *Science*, 2012, **335**, 59-64.
257. J. S. Baskin, H. Liu and A. H. Zewail, *Proceedings of the National Academy of Sciences*, 2014, **111**, 10479-10484.
258. E. Najafi, T. D. Scarborough, J. Tang and A. Zewail, *Science*, 2015, **347**, 164-167.
259. E. Knoesel, A. Hotzel and M. Wolf, *Physical Review B*, 1998, **57**, 12812-12824.
260. J. Lehmann, M. Merschdorf, W. Pfeiffer, A. Thon, S. Voll and G. Gerber, *Physical Review Letters*, 2000, **85**, 2921-2924.
261. A. Kubo, K. Onda, H. Petek, Z. Sun, Y. S. Jung and H. K. Kim, *Nano Letters*, 2005, **5**, 1123-1127.
262. M. Aeschlimann, M. Bauer, D. Bayer, T. Brixner, S. Cunovic, F. Dimler, A. Fischer, W. Pfeiffer, M. Rohmer, C. Schneider, F. Steeb, C. Strüber and D. V. Voronine, *Proceedings of the National Academy of Sciences*, 2010, **107**, 5329-5333.
263. M. Aeschlimann, T. Brixner, A. Fischer, C. Kramer, P. Melchior, W. Pfeiffer, C. Schneider, C. Strüber, P. Tuchscherer and D. V. Voronine, *Science*, 2011, **333**, 1723-1726.
264. M. Aeschlimann, T. Brixner, S. Cunovic, A. Fischer, P. Melchior, W. Pfeiffer, M. Rohmer, C. Schneider, Stru, x, C. ber, P. Tuchscherer and D. V. Voronine, *Selected Topics in Quantum Electronics, IEEE Journal of*, 2012, **18**, 275-282.
265. C. Lemke, C. Schneider, T. Leißner, D. Bayer, J. W. Radke, A. Fischer, P. Melchior, A. B. Evlyukhin, B. N. Chichkov, C. Reinhardt, M. Bauer and M. Aeschlimann, *Nano Letters*, 2013, **13**, 1053-1058.
266. C. Lemke, T. Leißner, A. Evlyukhin, J. W. Radke, A. Klick, J. Fiutowski, J. Kjelstrup-Hansen, H.-G. Rubahn, B. N. Chichkov, C. Reinhardt and M. Bauer, *Nano Letters*, 2014, **14**, 2431-2435.

267. M. Bauer, A. Marienfeld and M. Aeschlimann, *Progress in Surface Science*, 2015, **90**, 319-376.